The Arrangement of First- and Second-Sphere Water Molecules in Divalent Magnesium Complexes: Results from Molecular Orbital and Density Functional Theory and from Structural Crystallography

George D. Markham and Jenny P. Glusker*

Institute for Cancer Research, Fox Chase Cancer Center, 7701 Burholme Avenue, Philadelphia, Pennsylvania 19111

Charles W. Bock

Philadelphia University, Henry Avenue and Schoolhouse Lane, Philadelphia, Pennsylvania 19144, and Institute for Cancer Research, Fox Chase Cancer Center, 7701 Burholme Avenue, Philadelphia, Pennsylvania 19111

Received: January 11, 2002

The structures and binding enthalpies of a variety of gas-phase divalent magnesium ion hydrates containing up to 18 water molecules have been studied computationally. Second-order Møller−Plesset (MP2) perturbation theory and B3LYP hybrid density functional theory, using large basis sets containing both (multiple) polarization and diffuse functions, were employed. A comparison with experimental data is made by use of information on 36 $Mg[H_2O]_6^{2+}$ crystal structures listed in the Cambridge Structural Database. Computational studies indicate that $Mg[H_2O]_5^{2+}$ and $Mg[H_2O]_6^{2+}$ complexes with all the water molecules in the inner coordination sphere are lower in energy than structures with one or two of the water molecules placed in the second coordination sphere; these energy differences are larger for MP2 than for B3LYP calculations, when the same basis set is employed. Hydrated magnesium environments in crystal structures confirm the stability of the $Mg[H_2O]_6^{2+}$ grouping. A new model of a divalent magnesium ion complex with a total of 18 water molecules in two concentric shells of hydration is presented. In this model six water molecules are arranged octahedrally in the first coordination shell and 12 additional water molecules, hydrogen-bonded to those in the inner shell, fill the second shell. This new structure of $Mg[H_2O]_6^{2+}\cdot[H_2O]_{12}$ has an integrated hydrogen-bonding network in which water pentamers, composed of four second-shell water molecules and one first-shell water molecule, play a significant role. The geometry is derived from that of a pentagonal dodecahedral arrangement of water molecules enclosing an $Mg[H_2O]_6^{2+}$ octahedron. This model has S_6 symmetry and is calculated to be lower in energy than other forms of $Mg[H_2O]_6^{2+}\cdot[H_2O]_{12}$ previously described in the literature (Pavlov et al. *J. Phys. Chem. A.* **1998**, *102*, 219−228; Pye and Rudolph *J. Phys. Chem. A* **1998**, *102*, 9933−9943). The structure of $Mg[H_2O]_6^{2+}\cdot[H_2O]_{12}$ presented here provides additional insight into the importance of the water dipole moment in controlling the orientation of the water molecules in the first coordination shell and of water−water hydrogen bonding in controlling the orientation of water molecules in the second shell. These factors are also evident in crystal structures containing the $Mg[H_2O]_6^{2+}$ octahedron; in particular, a neutron diffraction study (Vanhouteghem, Lenstra, and Schweiss *Acta Crystallogr*. **1987**, *B43*, 523−528) showed that first-shell water molecules have the magnesium ion within 10° of the plane of each water molecule.

Introduction

The study of hydrated gas-phase metal ions provides a link between the intrinsic chemistry of the isolated ion and its chemistry in solution.[1,2] Experimental and computational studies have provided a wealth of data on the structures and stabilities of a variety of singly charged metal ion-water complexes.[3−27] In many biochemical systems, however, doubly charged metal ions, e.g., Mg^{2+}, Ca^{2+}, and Zn^{2+}, are of paramount importance and therefore there has been substantial interest in their individual hydration characteristics.[28] While doubly charged metal ions abound in aqueous solution, the preparation of their hydrated complexes, $M[H_2O]_n^{2+}$, in the gas-phase involves a host of technical problems,[29] and much of the data accumulated for these complexes have been obtained from computational studies.[30−67] Recent advances in mass spectrometry, however, have shown that $M[H_2O]_n^{2+}$ complexes can be prepared and studied by ion transfer from solution to the gas-phase using electrospray or thermospray techniques,[68,69] and results for a number of metal ions have been reported by Kebarle and co-workers[70−73] and by Williams and co-workers.[74,75] Similar complexes have also been generated directly from metal vapors using the novel "pick up" technique developed by Stace and co-workers.[29,76−79]

Divalent magnesium ions, which have a high charge-to-radius ratio, are (with Ca^{2+}) among the most common divalent cations in biological systems[11] and, as such, a variety of their gas-phase complexes have attracted attention as models. Results of experimental and computational studies agree that the first coordination shell of hydrated Mg^{2+} is completed with six water molecules,[30,31,39,43,45,80−84] and that the arrangement of these

* To whom correspondence should be addressed. Telephone: 215-728-2220. Fax: 215-728-2863. E-mail: JP_Glusker@fccc.edu.

10.1021/jp020078x CCC: $22.00
Published on Web 04/24/2002

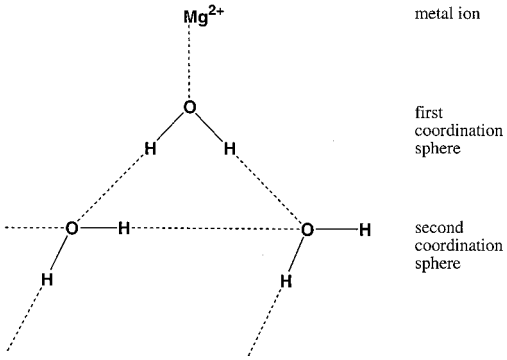

Figure 1. Diagram of the first two coordination shells (spheres) of water molecules around a divalent magnesium cation. Only one of the six water molecules in the first shell is shown here. Note the symmetrical orientation of the water molecule in the first shell (the dipole moment of the water being oriented toward the magnesium ion), and the very different arrangement of water molecules in the second sphere (where hydrogen bonding is paramount).

water molecules is generally regular, with the oxygen atoms at the corners of an octahedron. The global minimum on the potential energy surface (PES) of an isolated $Mg[H_2O]_6^{2+}$ complex has T_h symmetry.[30,31,39,43] A number of other hexahydrated divalent metal ion complexes, e.g., $Cd[H_2O]_6^{2+}$ and $Mn[H_2O]_6^{2+}$, appear to have similar structures.[12,40] In contrast, the global energy minimum for the hexahydrated complex of the smaller divalent beryllium ion is of the form $Be[H_2O]_4^{2+}\cdot[H_2O]_2$, in which there are four water molecules in the first shell and two in the second shell.[37,39,55] For hexahydrated Zn^{2+}, complexes of the form $Zn[H_2O]_6^{2+}$, $Zn[H_2O]_5^{2+}\cdot[H_2O]$, and $Zn[H_2O]_4^{2+}\cdot[H_2O]_2$ are relatively close in energy, and it is not yet clear which structure is the global minimum on the PES.[30,34,54]

The cation−water interactions in $Mg[H_2O]_6^{2+}$ are primarily electrostatic in origin, with the water dipoles directed toward the central magnesium ion (see Figure 1); none of the natural bond orbitals in $Mg[H_2O]_6^{2+}$ are classified as Mg−O bonding orbitals.[85] Interestingly, some hexahydrated monovalent metal ion complexes, e.g., $Na[H_2O]_6^{+}$, are found to have low-energy conformers in which the metal ion is sandwiched between two water trimers (S_6 symmetry).[14,21] These structures are apparently a result of relatively weak cation−water interactions which increase the significance of hydrogen bonding interactions.

The number of water molecules that complete the second hydration sphere of Mg^{2+} has been estimated in a variety of studies to be approximately 12,[80,83,84,86,87] but this number is much less certain. For example, in a recent molecular dynamics simulation Martinez et al.[45] found a second shell hydration number for Mg^{2+} of 13. Only recently, however, has it become possible to use high-level calculations to investigate the structure of hydrated metal ion complexes where there are a significant number of water molecules in the second coordination shell.[30,57] Pavlov et al., for example, reported a conformer of $Mg[H_2O]_6^{2+}\cdot[H_2O]_{12}$ in which each water molecule in the second shell is hydrogen bonded to one water molecule in the first shell and there is no hydrogen bonding between second shell water molecules;[30] their structure, optimized using density functional theory (DFT) at the B3LYP/LANL2DZ computational level, has (nearly) T_h symmetry. Results from a frequency analysis were not reported in their study.[30] A subsequent investigation of Mg^{2+} hydration by Pye and Rudolph[57] involved a version of the Pavlov et al.[30] structure in which T_h symmetry was enforced during the calculation at the HF/6-31G*//HF/6-31G* level. They found that this structure was not a local minimum on the PES at this computational level. By desymmetrizing along the highest frequency mode of this structure, they found a novel local minimum on the PES in which the second-sphere water molecules are arranged in four groups of hydrogen-bonded trimers attached to alternate faces of the $Mg[H_2O]_6^{2+}$ octahedron; the second-shell trimers are not hydrogen bonded to each other. Hartree−Fock frequency analysis of this structure provided a reasonable description of the MgO_6 vibrational modes observed in the experimental Raman spectroscopic data of magnesium perchlorate and chloride solutions.[57] Furthermore, the new conformer was some 30 kcal/mol *lower* in energy than the structure proposed by Pavlov et al.[30,57] As we will show, however, neither of these conformers appears to be the global minimum on the PES of Mg^{2+} surrounded by 18 water molecules.

The present work explores the structure and binding enthalpies of a variety of gas-phase divalent magnesium complexes containing up to 18 water molecules. The relatively weak hydrogen bonding between water molecules in these complexes, in conjunction with the large electrostatic ion−water interaction, provides a formidable problem for computational studies. We have used both Møller−Plesset perturbation theory and density functional theory (DFT) with large basis sets in this investigation. Comparisons of results are made with data on water organization around magnesium ions in crystal structures listed in the Cambridge Structural Database.[88]

Computational Methods

The complexes that we studied by computational methods included $Mg[H_2O]^{2+}$, $Mg[H_2O]_5^{2+}$, $Mg[H_2O]_4^{2+}\cdot[H_2O]$, $Mg[H_2O]_6^{2+}$, $Mg[H_2O]_5^{2+}\cdot[H_2O]$, $Mg[H_2O]_4^{2+}\cdot[H_2O]_2$, $Mg[H_2O]_6^{2+}\cdot[H_2O]$, and $Mg[H_2O]_6^{2+}\cdot[H_2O]_{12}$. Optimizations were initially carried out using the highly efficient, correlated, gradient-corrected Becke−Perdew (BP) method with the numerical DN** basis set (implemented in Spartan 5.0).[89−91] The numerical DN** basis set includes polarization functions on all atoms but no explicit diffuse functions. Frequency analyses using Spartan 5.0 can only be performed numerically and, for many of these weakly bound complexes, this is not sufficiently reliable for our purposes.[89] Therefore, optimizations and frequency analyses were also performed using the GAUSSIAN 94[92] and 98[93] series of programs with DFT at the B3LYP/6-31+G** or B3LYP/6-311++G** level[91,94,95] and, where possible, using second-order Møller−Plesset (MP2) perturbation theory[96] at the MP2(FULL)/6-311++G** level in order to compare methodological effects on the predicted geometrical parameters.[97] To evaluate more accurately the energy separation between different forms of these complexes, e.g., $Mg[H_2O]_6^{2+}$ and $Mg[H_2O]_5^{2+}\cdot[H_2O]$, and their binding energies, single point calculations were performed at the B3YLP/6-311++G**, B3LYP/6-311++G(2d,2p), B3LYP/6-311++G(3df,3pd), MP2(FC)/6-31+G*, MP2(FULL)/6-311++G**, and MP2(FULL)/6-311++G(2d,2p) levels using GAUSSIAN 94 and 98[92,93] on a variety of computers. For a few of the smaller complexes we also performed single-point coupled cluster (CC) calculations at the CCSDT(FULL)/6-311++G(3df,3pd) level, which includes both single and double excitations and a perturbational estimate of connected triple excitations.[98] These single-point calculations use large basis sets, which are needed to provide a reasonable description of the multipole moments and polarizability of water;[30] diffuse functions are important when interactions with oxygen-containing systems are present.[30] Atomic charges were obtained when possible using natural population analyses (NPA), and the wave functions were analyzed with the help of natural bond orbitals (NBOs).[99−101] Previous studies have shown that including basis

TABLE 1: Geometrical Parameters[a] of the Monohydrate $Mg[H_2O]^{2+}$ Calculated at Various Computational Levels

computational level	Mg−O (Å)	O−H (Å)	∠HOH (deg)
A. Pure DFT[b]			
local density approximation (LDA)[106]			
SVWN5/6-311++G(d,p)	1.922	0.991	106.0
SVWN5/6-311++G(2d,2p)	1.902	0.989	106.0
SVWN5/6-311++G(3df,3pd)	1.892	0.989	105.7
PW91[108,188−191]	1.885	0.990	105.8
generalized gradient approximation (GGA)[91,115,116]			
BLYP/6-311++G(d,p)	1.957	0.989	106.0
BLYP/6-311++G(2d,2p)	1.938	0.987	106.1
BLYP/6-311++G(3df,3pd)	1.929	0.987	105.8
PBE[117,118]	1.918	0.986	105.7
B. Hybrid DFT[95]			
B3LYP/6-311++G(d,p)	1.942	0.980	105.8
B3LYP/6-311++G(2d,2p)	1.924	0.978	106.1
B3LYP/6-311++G(3df,3pd)	1.914	0.978	105.8
C. Hartree−Fock (HF)			
HF/6-311++G(d,p)	1.939	0.956	105.8
HF/6-311++G(2d,2p)	1.919	0.957	106.1
HF/6-311++G(3df,3pd)	1.907	0.957	105.8
D. Møller−Plesset Perturbation Theory (MP)[96]			
MP2(FULL)/6-311++G(d,p)	1.957	0.976	105.1
MP2(FULL)/6-311++G(2d,2p)	1.936	0.973	105.4
MP2(FULL)/6-311++G(3df,3pd)	1.920	0.974	105.0
MP4SDTQ(FULL)/6-311++G(d,p)	1.957	0.976	105.0
MP4SDTQ(FULL)/6-311++G(2d,2p)	1.935	0.973	105.5
MP4SDTQ(FULL)/6-311++G(3df,3pd)	1.919	0.974	105.0

[a] At the BP/DN** computational level, Mg−O = 1.937 Å, O−H = 0.990 Å, and ∠HOH = 105.2°. [b] The program NRLMOL was used for the DFT methods PW91 and PBE.[109,111]

set superposition errors for Mg^{2+} complexes do not necessarily improve the accuracy of the results;[31] hence this correction was not incorporated into the binding energies reported in this work.

Cambridge Structural Database Analyses

The Cambridge Structural Database (CSD, April 2001 version)[88] was searched for all published crystal structures containing $Mg[H_2O]_6^{2+}$ ions by use of the program Quest3D that is connected with the database. A master file of three-dimensional coordinates and bibliographic references of crystal structures containing this grouping was obtained from this search. Some crystal structures were eliminated from the search because they contained disorder, high symmetry, problems with hydrogen atom locations, and/or the crystallographic *R* factor was high (greater than 0.10). The total structures were viewed by use of the graphics program ICRVIEW[102] and the metal ion coordination geometry was evaluated for each structure. Analysis of metric details of coordination geometry were done by use of the program BANG[103] with output data from the CSD as input.

Results

A variety of hydrated Mg^{2+} complexes with water molecules in the first and second hydration shells were studied at several computational levels using both DFT and Møller−Plesset methods. The resulting total molecular energies of these complexes are given in Table 1S. Thermal corrections to 298K and entropies calculated at the B3LYP/6-311++G**//B3LYP/6-311++G** level are given in Table 2S. Individual complexes will now be described in order of increasing size.

$Mg[H_2O]^{2+}$. The monohydrate, $Mg[H_2O]^{2+}$, is planar with C_{2v} symmetry at all the computational levels we considered. Such a structure is indicative of a strong ion−dipole interaction, a common result for both mono- and divalent-metal ion monohydrates.[16,41] Although some electron density (0.03e) is transferred from the water ligand to the magnesium ion, the bonding is predominantly electrostatic; no formal Mg−O bonding orbital was identified among the NBOs. We performed a variety of optimizations on $Mg[H_2O]^{2+}$ using pure DFT (within the local density approximation (LDA) and the generalized gradient approximation (GGA)), hybrid DFT (B3LYP),[95,104,105] Hartree−Fock, and Møller−Plesset perturbative methods with several high-quality basis sets. The optimized geometrical parameters are listed in Table 1.[104−116] Since several important DFT methods, e.g., PBE,[117,118] are not implemented in GAUSSIAN 98, in a few cases we employed the program NRLMOL,[109−114] which has a basis set that was optimized specifically for use with DFT calculations and which gives atomic energies within a few millihartree of the completely numerical results. As can be seen from Table 1, the calculated Mg−O distance is rather sensitive to the inclusion of multiple polarization functions into the basis set. It should be noted that *for a given basis set*, B3LYP calculations consistently yield shorter Mg−O distances than MP2(FULL) calculations, and LDA methods give shorter Mg−O distances than GGA methods; MP4SDTQ(FULL) and MP2(FULL) calculations give almost identical Mg−O distances.

Calculated values of the hydration binding enthalpies, ΔH°_{298}, for $Mg[H_2O]^{2+}$ are listed in Table 2 at a variety of computational levels. The thermal corrections used for these calculations of ΔH°_{298} were obtained from B3LYP/6-311++G** frequency analyses with no scaling; alternatively, use of thermal corrections from MP2(FULL)/6-311++G** frequency analyses change the calculated binding enthalpies by less than 0.1 kcal/mol. The binding enthalpy of $Mg[H_2O]^{2+}$ is not particularly sensitive to the optimized geometry employed in the calculation (see Table 2). It is sensitive, however, to the method employed: binding enthalpies calculated using the B3LYP method are consistently greater than those calculated using the MP2(FULL) method when the same basis set is employed; see Table 2.

To gain further insight into the importance of the ion−dipole interaction in $Mg[H_2O]^{2+}$, we reoptimized this complex with the plane of the water molecule constrained to be perpendicular to the line connecting the magnesium ion and the oxygen atom in order to attenuate the ion−dipole interaction. At the B3LYP/6-311++G** computational level, the Mg−O bond length in this constrained structure is 0.163 Å longer than in the planar arrangement, and the structure is over 27 kcal/mol higher in energy.

$[H_2O]_2$ and $[H_2O]_3$. Before considering larger hydrated gas-phase Mg^{2+} complexes, some forms of which contain hydrogen-bonded water molecules, it is important to compare the DFT and MP2 treatments of such water−water interactions. This is particularly important in light of questions that have been raised about the ability of B3LYP calculations, for example, to yield reliable binding energies for some hydrogen-bonded complexes.[119] Small water clusters have been studied extensively using a multitude of computational methods.[120−134] Our intention here is only to summarize a few results for the water dimer and water trimer that are of direct importance for the description of hydrated Mg^{2+} complexes. The water dimer and (cyclic) trimer were optimized at the BP/DN**, B3LYP/6-31+G**, B3LYP/6-311++G**, and MP2(FULL)/6-311++G** levels and selected geometrical parameters are given in Table 3S. For both the dimer and (cyclic) trimer B3LYP calculations find the O···H hydrogen bond lengths and the O···O distances to be *shorter* than those obtained from MP2 optimizations *using the same basis set*. The observed O···O distance is 2.98 Å,[135] some 0.07 Å greater than calculated at the MP2(FULL)/6-311++G**

TABLE 2: Binding Enthalpies, ΔH°_{298} (kcal/mol), for Various Divalent Magnesium Hydrates

	BP/DN** optimized geometry[a]			B3LYP/6-311++G** optimized geometry[a]	MP2(FULL)/6-311++G** optimized geometry[a]
structure	BP/DN**	MP2(FC)/6-31+G* (MP2(FULL)/6-311++G**) [MP2(FULL)/6-311++G(2d,2p)]	(B3LYP/6-311++G**) [B3LYP/6-311++G(2d,2p)]	(B3LYP/6-311++G**) [B3LYP/6-311++G(2d,2p)] {B3LYP/6-311++G(3df,3pd)}	(MP2(FULL)/6-311++G**) [MP2(FULL)/6-311++G(2d,2p)] {MP2(FULL)/6-311++G(3df,3pd)} ⟨CCSDT(FULL)/6-311++G(3df,3pd)⟩
$Mg[H_2O]^{2+}$	+81.7	+79.9			
		(+77.0)[c]	(+80.9)	(+80.9)	(+77.1)[b]
		[+76.7]	[+80.6]	[+80.6]	[+76.8][b]
				{+79.7}	{+78.4}
					⟨+78.4⟩[b,c]
$Mg[H_2O]_4^{2+}\cdot[H_2O]$	+270.9[d]			(+281.8)[d]	(+278.0)[d]
				[+277.1][d]	[+273.5][d]
				{+278.6}[d]	{+278.2}[d]
$Mg[H_2O]_5^{2+}$	+274.6				
		(+283.8)	(+284.2)	(+285.2)	(+284.7)
		[+277.9]	[+279.3]	[+280.3]	[+278.9]
				{+281.4}	{+283.5}
$Mg[H_2O]_6^{2+}$	+300.8	+326.0			
		(+317.1)	(+313.0)	(+312.8)	(+316.8)
		[+308.9]	[+306.5]	[+306.4]	[+308.8]
				{+307.0}	{+313.7}
$Mg[H_2O]_5^{2+}\cdot[H_2O]$	+297.8[d]	(+308.4)[d]	(+308.5)[d]	(+310.3)[d]	(+310.2)[d]
		[+301.8][d]	[+302.3][d]	[+304.0][d]	[+303.7][d]
				{+305.2}[d]	{+308.7}[d]
$Mg[H_2O]_4^{2+}\cdot[H_2O]_2$	+291.1	(+298.4)[d]	(+301.5)[d]	(+307.8)[d]	(+304.2)[d]
		[+292.4][d]	[+294.8][d]	[+301.8][d]	[+299.1][d]
				{+303.2}[d]	{+304.1}[d]
$Mg[H_2O]_6^{2+}\cdot[H_2O]$	+320.8[e]	+346.3[e]			
	+316.2[d]	(+336.6)[e]	(+331.8)[e]	(+332.1)[e]	(+336.8)[e]
		(+331.5)[d]	(+327.4)[d]	(+332.9)[d]	(+337.4)[d]
		[+327.4][e]	[+324.4][e]	[+324.6][e]	
		[+328.9][d]	{+319.5}[d]	(+325.2)[d]	
				{+325.2}[e]	
				{+325.7}[d]	
$Mg[H_2O]_6^{2+}\cdot[H_2O]_{12}$	+473.7[f]	+532.7			
(PSS)		(+515.8)	(+497.1)		
			[+480.4]		
(PRC)	+462.6[g]	+540.7			
		(+512.8)	(+493.3)	(+494.7)[h]	
		[+495.9]	[+473.2]	[+474.7]	
				{+473.1}	
(this work)	+477.2[i]	+551.5[i]			
		(+520.9)[i]	(+499.6)[i]	(+501.4)[i,j,k]	
		[+503.6][i]	[+479.1][i]		

[a] The thermal corrections used to obtain ΔH°_{298} were from frequency analyses at the B3LYP/6-311++G**//B3LYP/6-311++G** computational level with no scaling. [b] The thermal corrections used to obtain ΔH°_{298} were from frequency analyses at the MP2(FULL)/6-311++G**//MP2(FULL)/6-311++G** computational level with no scaling. [c] At the CCSD(T)(FULL)/6-311++G**//MP2(FULL)/6-311++G** computational level the binding enthalpy is +76.8 kcal/mol.[41] [d] Second-shell water molecule(s) bound to two first-shell water molecules with two hydrogen bonds. [e] Second-shell water molecule(s) bound to one first-shell water molecule with a single hydrogen bond. [f] Pavlov et al.[30] report a value of 460.8 kcal/mol at the B3LYP/LANL2DZ//B3LYP/LANL2DZ level. [g] Pye and Rudolph report a value of 518.9 kcal/mol at the HF/6-31+G*//HF/6-31+G* level. [h] At the B3LYP/6-31+G**//B3LYP/6-31+G** computational level $\Delta H^\circ_{298} = 500.2$ kcal/mol. [i] The thermal corrections used to obtain ΔH°_{298} were from frequency analyses at the B3LYP/6-31+G**//B3LYP/6-31+G** computational level with no scaling; see Table 2S. [j] At the B3LYP/6-31+G**//B3LYP/6-31+G** computational level $\Delta H^\circ_{298} = 507.9$ kcal/mol. [k] The structure of $Mg[H_2O]_6^{2+}\cdot[H_2O]_{12}$ was only partially optimized at this computational level. Thus, the value of 501.4 kcal/mol for this binding energy is a lower bound.

TABLE 3: Comparison of the Energy Differences, ΔE (kcal/mol), between the Complexes $Mg[H_2O]_6^{2+}$, $Mg[H_2O]_5^{2+}\cdot[H_2O]$, and $Mg[H_2O]_4^{2+}\cdot[H_2O]_2$ and between the Complexes $Mg[H_2O]_5^{2+}$ and $Mg[H_2O]_4^{2+}\cdot[H_2O]$

structure	$Mg[H_2O]_5^{2+}$	$Mg[H_2O]_4^{2+}\cdot[H_2O]$	$Mg[H_2O]_6^{2+}$	$Mg[H_2O]_5^{2+}\cdot[H_2O]$	$Mg[H_2O]_4^{2+}\cdot[H_2O]_2$
		A. B3LYP/6-311++G(d,p) Geometry			
B3LYP/6-311++G(d,p)	+0.0	+3.3	0.0	+2.2	+4.5
		(+3.4)[a]		(+3.2)[a]	(+5.0)[a]
B3LYP/6-311++G(2d,2p)	+0.0	+3.0	0.0	+1.9	+4.0
		(+3.1)[a]		(+2.9)[a]	(4.5)[a]
B3LYP/6-311++G(3df,3dp)	+0.0	+2.6	0.0	+1.4	+3.3
		(+2.7)[a]		(+2.4)[a]	(+3.8)[a]
		B. MP2(FULL)/6-311++G(d,p) Geometry			
MP2(FULL)/6-311++G(d,p)	+0.0	+6.6	0.0	+6.2	+12.0
		(+6.7)[a]		(+7.2)[a]	(+12.5)[a]
MP2(FULL)/6-311++G(2d,2p)	+0.0	+5.3	0.0	+4.8	+9.2
		(+5.4)[a]		(+5.8)[a]	(+9.7)[a]
MP2(FULL)/6-311++G(3df,3dp)	+0.0	+5.2	0.0	+4.6	+9.1
		(+5.3)[a]		(+5.6)[a]	(+9.6)[a]

[a] Includes thermal corrections to 298 K from B3LYP/6-311++G** frequency analyses.

TABLE 4: Geometrical Parameters[a] of the Hexahydrate $Mg[H_2O]_6^{2+}$ Calculated at Various Computational Levels

computational level	Mg−O (Å)	O−H (Å)	∠HOH (deg)
	A. Pure DFT		
local density approximation (LDA)[106]			
SVWN5/6-311++G**	2.055	0.977	107.2
SVWN5/6-311++G(2d,2p)	2.045	0.976	107.2
SVWN5/6-311++G(3df,3pd)	2.042	0.976	107.0
generalized gradient approximation (GGA)[91,115,116]			
BLYP/6-311++G**	2.135	0.976	106.2
BLYP/6-311++G (2d,2p)	2.125	0.975	106.4
BLYP/6-311++G(3df,3pd)	2.123	0.975	106.1
	B. Hybrid DFT[95]		
B3LYP/6-311++G**	2.112	0.967	106.6
B3LYP/6-311++G(2d,2p)	2.102	0.965	106.7
B3LYP/6-311++G(3df,3pd)	2.100	0.965	106.5
	C. Hartree−Fock (HF)		
HF/6-311++G**	2.111	0.948	107.1
HF/6-311++G(2d,2p)	2.100	0.945	107.1
HF/6-311++G(3df,3pd)	2.098	0.945	107.1
	D. Møller−Plesset Perturbation Theory[96]		
MP2(FULL)/6-311++G**	2.103	0.965	105.7
MP2(FULL)/6-311++G(2d,2p)	2.092	0.962	106.1
MP2(FULL)/6-311++G(3df,3pd)	2.081	0.963	105.8

[a] At the BP/DN** computational level, Mg−O = 2.106 Å, O−H = 0.975 Å, ∠HOH = 106.1°.

level. Nevertheless, our calculated O···O distances are in good agreement with the extensive set of calculations reported by Estrin et al.[126]

The binding enthalpies calculated for the water dimer using the MP2(FULL) model are slightly *higher* than those calculated using the B3LYP model when the same basis set is employed; see Table 4S. Furthermore, this enthalpy difference increases slightly as the basis set becomes more complete. For the dimer, the calculated MP2(FULL)/6-311++G(2d,2p) and CCSDT-(FULL)/6-311++G(3df,3pd) binding enthalpies are both 3.6 kcal/mol, very close to the experimental value of 3.59 ± 0.5 kcal/mol,[136] while the B3LYP/6-311++G(2d,2p) and B3LYP/6-311++G(3df,3pd) binding enthalpies are *lower*, 3.2 and 3.0 kcal/mol respectively, at the edge of the experimental uncertainty. An interesting discussion of basis set superposition errors (BSSEs) for the water dimer has been given recently by Simon et al.[137] They concluded that DFT methods are less subject to BSSE than MP2 methods, and that DFT provides reliable results for hydrogen bonding in this case.

For the (cyclic) water trimer,[138,139] we also find higher values of the binding enthalpy at the MP2(FULL) level compared to that at the B3LYP level using either the 6-311++G** or 6-311++G(2d,2p) basis sets. Although no experimental result for this binding enthalpy is currently available, our calculations are in good agreement with the results obtained by Estrin et al.[126]

$Mg[H_2O]_5^{2+}$ and $Mg[H_2O]_4^{2+}\cdot[H_2O]$. There has been renewed interest in the various conformers of pentahydrated Mg^{2+} complexes because it has been suggested that at higher temperatures the structure of the pentahydrate is $Mg[H_2O]_4^{2+}\cdot[H_2O]$ rather than $Mg[H_2O]_5^{2+}$.[140] The lowest energy form of $Mg[H_2O]_4^{2+}\cdot[H_2O]$ has the second-shell water molecule hydrogen-bonded to two different inner-shell water molecules; the structure of $Mg[H_2O]_4^{2+}\cdot[H_2O]$ in which the second-shell water is hydrogen-bonded to only a single first-shell water molecule is approximately 2 kcal/mol *higher* in energy. B3LYP and MP2-(FULL) calculations find $Mg[H_2O]_5^{2+}$ *lower* in energy than $Mg[H_2O]_4^{2+}\cdot[H_2O]$ (see Tables 3 and 1S), in agreement with other calculations on these complexes at a variety of computational levels.[30,39] The predicted MP2(FULL) energy difference between these isomers, however, is consistently about double the B3LYP energy difference *using the same basis set*; see Table 3. It should also be noted that the calculated entropy of $Mg[H_2O]_4^{2+}\cdot[H_2O]$ is just slightly *smaller* than that of $Mg[H_2O]_5^{2+}$ at the B3LYP/6-311++G**//B3LYP/6-311++G** and MP2-(FULL)/6-311++G**//MP2(FULL)/6-311++G** levels; see

TABLE 5: Average Structural Parameters of 36 $Mg[H_2O]_6^{2+}$ Clusters Found in the Cambridge Structural Database[146−178]

refcode	Mg−O[a] (first) (Å)	Mg···H[b] (first)	δH[c] (Å)	Mg···O (second) (Å)	δH for each water molecule in second shell (Å)		no. of water molecules in second shell	Mg···O[d] (third) (Å)
CIRVAA01[e,152]	2.066	2.710	0.039	4.305			0	
ANAPHS[146]	2.058	2.61	0.11	4.246	0.93	0.95	2	6.70
AQMEDA[147]	2.076	2.63	0.07	4.296			0	
BADTEX01[148]	2.057	2.62	0.12	4.325	0.43		1	6.33
BADTEX10[148]	2.056	2.61	0.09	4.312	0.47		1	6.75
BIKPUG[149]	2.077	2.65	0.08	4.499			0	
CAWTID[150]	2.061	2.87	0.08	4.415	0.04		1	6.51
CIRVAA[151]	2.049	2.62	0.04	4.296			0	
DXMGHC10[153]	2.063	2.69	0.23	4.634			0	
FEDQUA[154]	2.073	2.63	0.15	4.374	0.06	0.55	2	6.30
FEDQUA01[155]	2.074	2.65	0.13	4.375	0.03	0.47	2	6.30
GATLUI[156]	2.066	2.62	0.04	4.283	0.42		1	5.71
GIJVEA[157]	2.053	2.48	0.07	4.300			0	
GOLPIG[158]	2.058	2.63	0.13	4.297	0.12	0.82	2	7.07
GOLPIG[158]	2.056	2.63	0.10	4.263	0.11	0.89	2	6.26
GUHHOG[159]	2.067	2.60	0.02	4.262	0.41		1	6.91
HAHWAO[160]	2.053	2.49	0.07	4.171	0.75		1	5.00
HETZUB[161]	2.074	2.61	0.13	4.203	0.49	0.81	2	6.29
HMTMGC10[162]	2.101	2.76	0.00	4.530			0	
KEQRAZ[163]	2.058	2.59	0.08	4.314	0.47		1	6.51
KIMNID[164]	2.060	2.65	0.10	4.365	0.25		1	5.99
MGCITD[165]	2.074	2.62	0.09	4.310	0.29	0.49	2	7.23
MGEDTA01[166]	2.062	2.60	0.04	4.443	0.04		1	5.93
MGNTSP[167]	2.060	2.58	0.07	4.188			0	
RATRIN[168]	2.065	2.51	0.26	4.220			0	
RIVCAA[169]	2.061	2.67	0.08	4.134			0	
SIMZUJ[170]	2.067	2.67	0.01	4.252	0.15		1	5.30
TEKBIU[171]	2.055	2.69	0.13	4.164	0.01		1	4.48
THIAMG10[172]	2.051	2.53	0.13	4.301	0.27	0.37	2	5.85
TOXDMG[173]	2.065	2.59	0.10	4.439			0	
VOPCEI[174]	2.058	2.60	0.03	4.260			0	
VUKMIX[175]	2.061	2.56	0.09	4.329	0.16		1	4.97
WIKXAP[176]	2.056	2.61	0.06	4.269	0.41		1	6.41
WIKXAP[176]	2.058	2.61	0.11	4.395	0.35	0.44	2	6.25
ZARMEK[177]	2.058	2.59	0.10	4.206	0.08	0.30	4	6.55
					0.21	0.30		
ZURWIS[178]	2.052	2.63	0.04	4.255	0.48	0.81	2	7.14
averages of averages	2.063	2.62	0.09	4.312	0.40			6.20

[a] Average Mg^{2+}−O distances per structure in inner (first) coordination shell. [b] Average distances per structure from Mg^{2+} to the hydrogen atoms of the water molecules in the inner coordination shell. [c] δH = average difference in Mg^{2+}···H distances for the two hydrogen atoms of a given water molecule. [d] Maximum Mg^{2+}···O distances for the third coordination shell. [e] Neutron-diffraction study.

Table 2S. These results suggest that the conversion from an inner-shell coordination number of 5 to 4 is entropically, as well as enthalpically, unfavorable.

$Mg[H_2O]_6^{2+}$, $Mg[H_2O]_5^{2+}\cdot[H_2O]$, and $Mg[H_2O]_4^{2+}\cdot[H_2O]_2$. It has generally been inferred that six water molecules are required to complete the first coordination shell surrounding Mg^{2+}, and this is supported by several observations. First, all the crystal structures in the Cambridge Structural Database (CSD)[88] that contain a hexahydrated Mg^{2+} ion have all six water molecules in the inner shell (octahedral coordination).[38] Second, solutions containing Mg^{2+} ions have been widely investigated using X-ray diffraction methods and these experiments have consistently found the inner shell surrounding these ions to contain six water molecules.[80,82−84,86,141−145] Third, computational studies of gas-phase hexahydrated Mg^{2+} ions have been reported at several computational levels,[30,33,38,43] and the global minimum on the potential energy surface (PES) has been identified as $Mg[H_2O]_6^{2+}$ with T_h symmetry. In this arrangement, the water dipoles point directly toward the magnesium ion (see Figure 1), indicative of a strong metal ion−water dipole interaction that also minimizes the water−water repulsion. Interestingly, blackbody infrared radiative dissociation (BIRD) experiments have recently suggested that there are two isomeric forms of hexahydrated divalent magnesium complexes in the gas phase: presumably $Mg[H_2O]_6^{2+}$ at lower temperatures and $Mg[H_2O]_4^{2+}\cdot[H_2O]_2$ at higher temperatures.[74] Only one hexahydrate, $M[H_2O]_6^{2+}$, was found for the other alkaline earths (M = Ca, Sr, and Ba).[74]

We considered three forms of hexahydrated magnesium: $Mg[H_2O]_6^{2+}$, $Mg[H_2O]_5^{2+}\cdot[H_2O]$, and $Mg[H_2O]_4^{2+}\cdot[H_2O]_2$. Optimized geometrical parameters of $Mg[H_2O]_6^{2+}$ (T_h symmetry) at a variety of computational levels are given in Table 4; here it is evident that the calculated Mg−O distances are much less sensitive to an increase in the size of the basis set than was the case for the monohydrate, $Mg[H_2O]^{2+}$ (compare Tables 1 and 4). Frequency analyses at the B3LYP/6-311++G** and MP2(FULL)/6-311++G** levels confirm that this form of $Mg[H_2O]_6^{2+}$ is a local minimum on the PES; the calculated frequencies of $Mg[H_2O]_6^{2+}$ are listed in Table 5S at several computational levels.[57] In Table 2 we list the binding enthalpies of $Mg[H_2O]_6^{2+}$ calculated from a variety of methods. The B3LYP calculations give *lower* binding enthalpies for $Mg[H_2O]_6^{2+}$ than do the corresponding MP2 calculations when *the same basis set is used*. For some basis sets the difference is rather large, e.g., 6.7 kcal/mol (2%), using the 6-311++G(3df,3pd) basis set.

The geometries of 36 $Mg[H_2O]_6^{2+}$ clusters found in the CSD[88,146−178] are given in Table 5. The average Mg−O distance

is 2.063 Å and the average distance from the Mg^{2+} to the hydrogen atoms bonded to the water oxygen atoms is 2.62 Å (2.710 Å for the one neutron-diffraction study, CIRVAA01).[152] None of these structures have hydrogen bonding between the six water molecules in the inner coordination sphere; these water molecules have their dipole moments pointing at the magnesium ion so that the two Mg···H distances are about the same for each water molecule (average deviation, δH, is 0.09 Å; see Table 5).

For the lowest-energy forms that we found of the two-shell hexahydrates $Mg[H_2O]_5^{2+}\cdot[H_2O]$ and $Mg[H_2O]_4^{2+}\cdot[H_2O]_2$, the water molecules in the second shell are hydrogen-bonded to *two* water molecules in the first shell. Our MP2(FULL) and B3LYP calculations all find $Mg[H_2O]_6^{2+}$ to be *lower* in energy than either $Mg[H_2O]_5^{2+}\cdot[H_2O]$ or $Mg[H_2O]_4^{2+}\cdot[H_2O]_2$, in agreement with various other calculations.[30,38,39] As can be seen from Table 3, however, B3LYP calculations find relatively small energy differences among these three hexahydrates, and this seems to be endemic to many DFT methods. For example, we performed optimizations of $Mg[H_2O]_6^{2+}$ and $Mg[H_2O]_5^{2+}\cdot[H_2O]$ at the SVWN5 (LDA) level using the 6-311++G**, 6-311++G(2d,2p), and 6-311++G(3df,3pd) basis sets. These calculations find $Mg[H_2O]_5^{2+}\cdot[H_2O]$ to be *lower* in energy than $Mg[H_2O]_6^{2+}$ by 0.2, 0.3 and 1.1 kcal/mol, respectively. The corresponding BLYP (GGA) optimizations find $Mg[H_2O]_6^{2+}$ to be *lower* in energy, but by less than 1 kcal/mol. Based on the observed biochemical behavior of Mg^{2+} complexes, it would be difficult to rationalize such a low energy difference between $Mg[H_2O]_6^{2+}$ and $Mg[H_2O]_5^{2+}\cdot[H_2O]$. Clearly, MP2(FULL) calculations show a significantly stronger preference than DFT calculations for an inner-shell coordination number of 6.

We also note that the NPA charges on the magnesium ion in $Mg[H_2O]_6^{2+}$, $Mg[H_2O]_5^{2+}\cdot[H_2O]$, and $Mg[H_2O]_4^{2+}\cdot[H_2O]_2$ are +1.82e, +1.83e, and +1.84e respectively using the B3LYP/6-311++G** computational level. Thus, the more electron density that is transferred to the magnesium ion from the water ligands, the lower the total molecular energy of the hexahydrate.

Calculated values of ΔH°_{298} for the reaction

$$Mg[H_2O]_6^{2+} \rightarrow Mg[H_2O]_5^{2+} + H_2O \qquad (1)$$

are listed in Table 6 at the several computational levels; the experimental value of ΔH°_{298} for this reaction is 24.6 kcal/mol.[179] At the B3LYP/6-311++G(3df,3pd)//B3LYP/6-311++G** computational level the predicted value of ΔH°_{298} is 25.6 kcal/mol, in excellent agreement with the experimental result; the corresponding MP2(FULL) value is nearly 5 kcal/mol higher. The calculated value of ΔS for this reaction is quite large 40.9 [39.5] cal/(mol K) at the B3LYP/6-311++G** [MP2(FULL)6-311++G**] levels; the experimental value of ΔS is only 29.1 cal/(mol K).[179] It may be noted that the conversion from an inner-shell coordination number of 6 to either 5 or 4 is entropically favored at the B3LYP/6-311++G** computational level; see Table 2S.

$Mg[H_2O]_6^{2+}\cdot[H_2O]$. The heptahydrate of Mg^{2+}, presumably with one water molecule in the second coordination sphere, is the largest complex for which experimental thermochemical data for its formation are available.[73] The energetics of binding the seventh water molecule reflect both its electrostatic interaction with the Mg^{2+} ion and its hydrogen bonding to water molecules in the first coordination sphere. Optimizations of $Mg[H_2O]_6^{2+}\cdot[H_2O]$ at the BP/DN** level find that the form in which the second-shell water molecule is hydrogen-bonded to a single water molecule in the first coordination shell is *lower* in energy than the form in which the second-shell water molecule is hydrogen-bonded to two water molecules; see Table 1S. However, optimizations at the B3LYP/6-311++G** computational level and subsequent single-point calculations find the structure of the doubly hydrogen-bonded form to be about 1 kcal/mol *lower* in energy than the single hydrogen-bonded form; MP2(FULL)/6-311++G** optimizations also find the doubly bridged form lower in energy, but these structures were too large for us to perform frequency analyses at this MP2 level. The B3LYP/6-311++G** optimized structures of both of these forms are shown in Figures 2a,b. The distances between the second- and (closest) first-shell water molecules for the single hydrogen-bonded form are 1.649 for H···O and 2.648 Å for O···O at the B3LYP/6-311++G** level; these distances are 0.284 and 0.252 Å *shorter* than that found for an isolated water dimer; see Table 3S in the Supporting Information. The average Mg−O distance for the five water molecules that are not involved in the hydrogen bonding to the second-shell water molecule is 2.118 Å, marginally larger than this distance in the $Mg[H_2O]_6^{2+}$ complex, 2.112 Å, whereas the Mg−O distance for the inner-shell water molecule involved in the hydrogen bonding is smaller, 2.063 Å. The Mg···O distance for the second-shell water molecule is 4.264 Å. For the doubly hydrogen-bonded structure, both the two H···O distances, 1.851 and 1.842 Å, and the two O···O distances, 2.787 and 2.768 Å, are longer than the corresponding distances for the single hydrogen-bonded form, whereas the Mg···O distance is significantly shorter, 3.934 Å.

The net binding enthalpy for the seven water molecules in $Mg[H_2O]_6^{2+}\cdot[H_2O]$ is found to be about 325 kcal/mol for either form at the B3LYP/6-311++G(3df,3pd)//B3LYP/6-311++G** computational level (see Table 2); Pavlov et al. have reported a similar value, 321.9 kcal/mol.[30] Calculated enthalpy values for the reaction

$$Mg[H_2O]_6^{2+}\cdot[H_2O] \rightarrow Mg[H_2O]_6^{2+} + H_2O \qquad (2)$$

which is a measure of the binding of the first water molecule in the second shell to the hexahydrated magnesium complex $Mg[H_2O]_6^{2+}$, are given in Table 6. The values of ΔH°_{298} for this dehydration process are +18.2 and +18.7 kcal/mol for the single and double hydrogen-bonded forms, respectively, at the B3LYP/6-311++G(3df,3pd)//B3LYP/6-311++G** computational level. The recent experimental measurements of Peschke et al.[73] using electrospray ionization, ESI, in conjunction with mass spectrometry give a slightly higher value for ΔH°_{298}, 20.3 kcal/mol. Peschke et al.[73] also reported a value of 25.3 cal/(mol K) for the entropy change, ΔS, in reaction 2. Using the entropies listed in Table 2S, the calculated values of ΔS for reaction 2 are 22.2 and 25.7 cal/(mol K) for the single and double hydrogen-bonded forms, respectively. These B3LYP calculations suggest that it is the double hydrogen-bridged structure that was formed in the ESI experiments.

We calculated the interaction energy between a Mg^{2+} ion and a single water molecule at the position and geometry of the second-shell water molecule from the B3LYP/6-311++G** optimized geometry of the single hydrogen-bonded form of $Mg[H_2O]_6^{2+}\cdot[H_2O]$. The binding energy of this water molecule, in the absence of any screening from the inner-shell water molecules, is almost the same as the binding energy of this water molecule in the presence of the six water molecules. It may be noted that in both forms of $Mg[H_2O]_6^{2+}\cdot[H_2O]$, where second-shell water−water interactions are absent, the dipole moment of the second-shell water molecule is directed toward the central Mg^{2+} ion, e.g., the angle between the plane of the water molecule and a line connecting the magnesium and oxygen

TABLE 6: Calculated Enthalpy Changes, ΔH°_{298} (kcal/mol), for Various Reactions Involving Hydrated Magnesium Divalent Complexes

	BP/DN** Optimized Geometry[a]			B3LYP/6-311++G** Optimized Geometry[a]	MP2(FULL)/6-311++G** Optimized Geometry[a]
reaction	BP/DN**	MP2(FC)/6-31+G* (MP2(FULL)/6-311++G**) [MP2(FULL)/6-311++G(2d,2p)]	(B3LYP/6-311++G**) [B3LYP/6-311++G(2d,2p)]	(B3LYP/6-311++G**) [B3LYP/6-311++G(2d,2p)] {B3LYP/6-311++G(3df,3pd)}	(MP2(FULL)/6-311++G**) [MP2(FULL)/6-311++G(2d,2p)] {MP2(FULL)/6-311++G(3df,3pd)}
$Mg[H_2O]_6^{2+} \rightarrow Mg[H_2O]_5^{2+} + H_2O$	+29.2				
(experimental $\Delta H^\circ_{298} = 24.6$ kcal/mol)[67]		(+33.2) [30.9]	(+28.7) [+27.2]	(+27.6) [+26.1]	(+32.0) [+30.0]
$Mg[H_2O]_6^{2+}\cdot[H_2O] \rightarrow Mg[H_2O]_6^{2+} + H_2O$	+20.0[b]	+20.3[b]			
(experimental $\Delta H^\circ_{298} = 20.3$ kcal/mol)[67]	+15.4[c]	(+19.6)[b] (+14.4)[c] [+18.6][b] [+13.8][c]	(+18.9)[b] (+14.5)[c] [+18.0][b] [+13.1][c] {+18.2}[b] {+18.7}[c]	(+19.2)[b] (+20.1)[c] [+18.2][b] [+18.8][c]	(+20.0)[b] (+20.6)[c]
$Mg[H_2O]_6^{2+}\cdot[H_2O]_{12} \rightarrow Mg[H_2O]_6^{2+} + 12(H_2O)$	+161.8	+214.7			
(PRC)		(+195.8) [+187.1]	(+180.4) [+166.7] {+166.1}	(+181.9) [+168.3]	
$Mg[H_2O]_6^{2+}\cdot[H_2O]_{12} \rightarrow Mg[H_2O]_6^{2+} + 4(H_2O)_3$	+118.7	+155.4			
(PRC)		(+147.6) [+141.2]	(+132.7) [+125.8] {+125.0}	(+130.7) [+125.8]	
$Mg[H_2O]_6^{2+}\cdot[H_2O]_{12} \rightarrow Mg[H_2O]_6^{2+} + 12(H_2O)$	+176.3	+225.5			
(this work)		(+203.8) [+194.7]	(+186.6) [+172.5]	(+185.4)[d]	

[a] Thermal corrections used to obtain ΔH°_{298} were from B3LYP/6-311++G** frequency analysis with no scaling. [b] Second-shell water molecule is hydrogen-bonded to one first-shell water molecule. [c] Second-shell water molecule is hydrogen-bonded to two first-shell water molecules. [d] Calculated at the B3LYP/6-31+G**//B3LYP/6-31+G** computational level.

atoms in the single hydrogen-bonded structure is 89.6° for the B3LYP/6-311++G** optimized geometry. For the doubly bridged form the net NPA charge on the $Mg[H_2O]_6^{2+}$ moiety is slightly less than +2e, +1.95e at the B3LYP/6-311++G** level, although the positive charge remains primarily concentrated on the magnesium ion, +1.82e.

$Mg[H_2O]_6^{2+}\cdot[H_2O]_{12}$. Previous studies have found that about 12 water molecules are required to complete the second hydration sphere around a divalent magnesium ion.[80] Thus, we considered a variety of conformations of hydrated Mg^{2+} ions with six water molecules in the inner shell hydrogen bonded to 12 water molecules in the outer shell. Detailed analyses of the 34 crystal structures in the CSD that contain $Mg[H_2O]_6^{2+}$ clusters[146−178] provide some information about the second coordination shell; this shell was considered as consisting of atoms that were hydrogen bonded to the six inner-shell water molecules. In 24 cases these second-shell atoms were only oxygen atoms. One crystal structure contained four water molecules in the magnesium second coordination shell, but others contained two at most. The other hydrogen-bonded atoms were from counterions or solvent (other than water) in the crystal structure. The second shell (86% O, 8% N, 5% Cl, 0.4% Br) was found to be at an average distance of 4.312 Å from the magnesium ion with a variation between 4.164 and 4.634 Å. For those crystal structures with water molecules in the second shell, the Mg···H distances for a given second-shell water molecule may vary considerably (see Table 5); often one O−H bond lies along the surface of the second coordination shell, while the other O−H bond projects out, presumably to aid in bonding to the third coordination sphere at about 6 Å from the magnesium ion.

These 18-water complexes were too large for us to optimize at the MP2(FULL)/6-311++G** level and we therefore restricted optimizations to various DFT computational levels. For our calculations we initially considered the model of $Mg[H_2O]_6^{2+}\cdot[H_2O]_{12}$ first reported by Pavlov et al.,[30] which we denote here as the PSS conformer. Their optimization was performed using the B3LYP computational level with the pseudopotential LANL2DZ basis set;[30] no symmetry constraints were employed.[30] Using the Cartesian coordinates of their final structure as input, we reoptimized this complex at the BP/DN** level with no symmetry constraints. The resulting structure is shown in Figure 3a and Figure 1S in Supporting Information. It is very similar to that reported by Pavlov et al.[30] in that it has 12 water molecules in the second hydration shell, each of which is hydrogen-bonded to one of the water molecules in the first shell, and there is no hydrogen bonding between water molecules in the second shell. In this structure of $Mg[H_2O]_6^{2+}\cdot[H_2O]_{12}$, which has nearly T_h symmetry, the 24 hydrogen atoms from the water molecules in the second shell are all essentially the same distance away from the central magnesium ion. The arrangement of the six inner-shell water molecules is similar to that found in the $Mg[H_2O]_6^{2+}$ complex, although the average Mg−O distance of 2.097 Å is approximately 0.015 Å smaller than that found in the isolated hexahydrate. This reduction in length is consistent with the results reported by Pavlov et al.[30] at the B3LYP/LANL2DZ computational level. The average Mg···O distance for the outer-shell waters is 4.454 Å, while the average O···O distance between an inner-shell water molecule and its two closest outer-shell water molecules is 2.813 Å; the corresponding values at the B3LYP/LANL2DZ level are 4.409 and 2.74 Å, respectively.[30] It is interesting that the average calculated O···O distance for this arrangement of $Mg[H_2O]_6^{2+}\cdot[H_2O]_{12}$ is significantly shorter than the corresponding O···O distance for an isolated water dimer at the BP/DN** level, 2.887 Å. Although no direct experimental determinations of the structure of an isolated $Mg[H_2O]_6^{2+}\cdot[H_2O]_{12}$ complex are currently available, we find from studies of the crystallographic literature that the mean O···O distance between first- and second-sphere oxygen atoms in a variety of magnesium compounds is 2.784(6) Å.

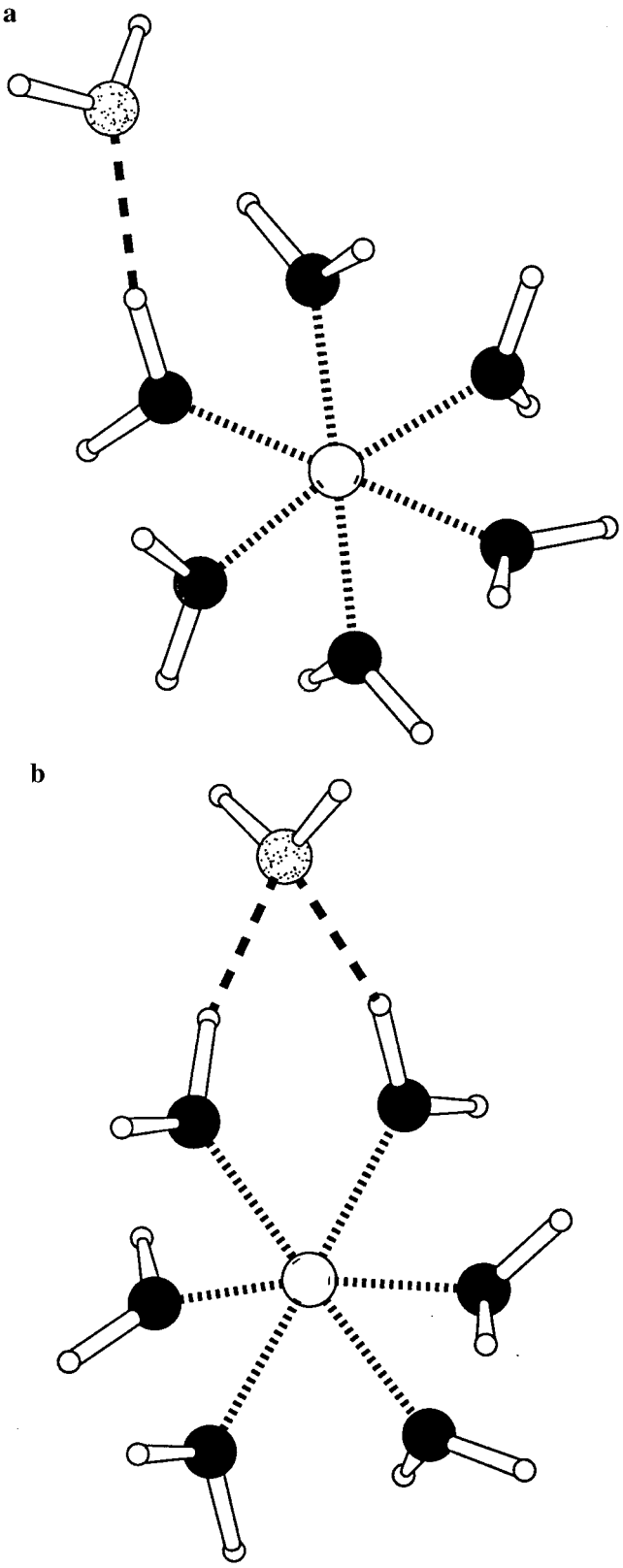

Figure 2. Structures of the (a) single and (b) doubly hydrogen-bridged $Mg[H_2O]_6^{2+}\cdot[H_2O]$ complex. In this and all subsequent figures oxygen atoms in the first shell are black, in the second shell speckled.

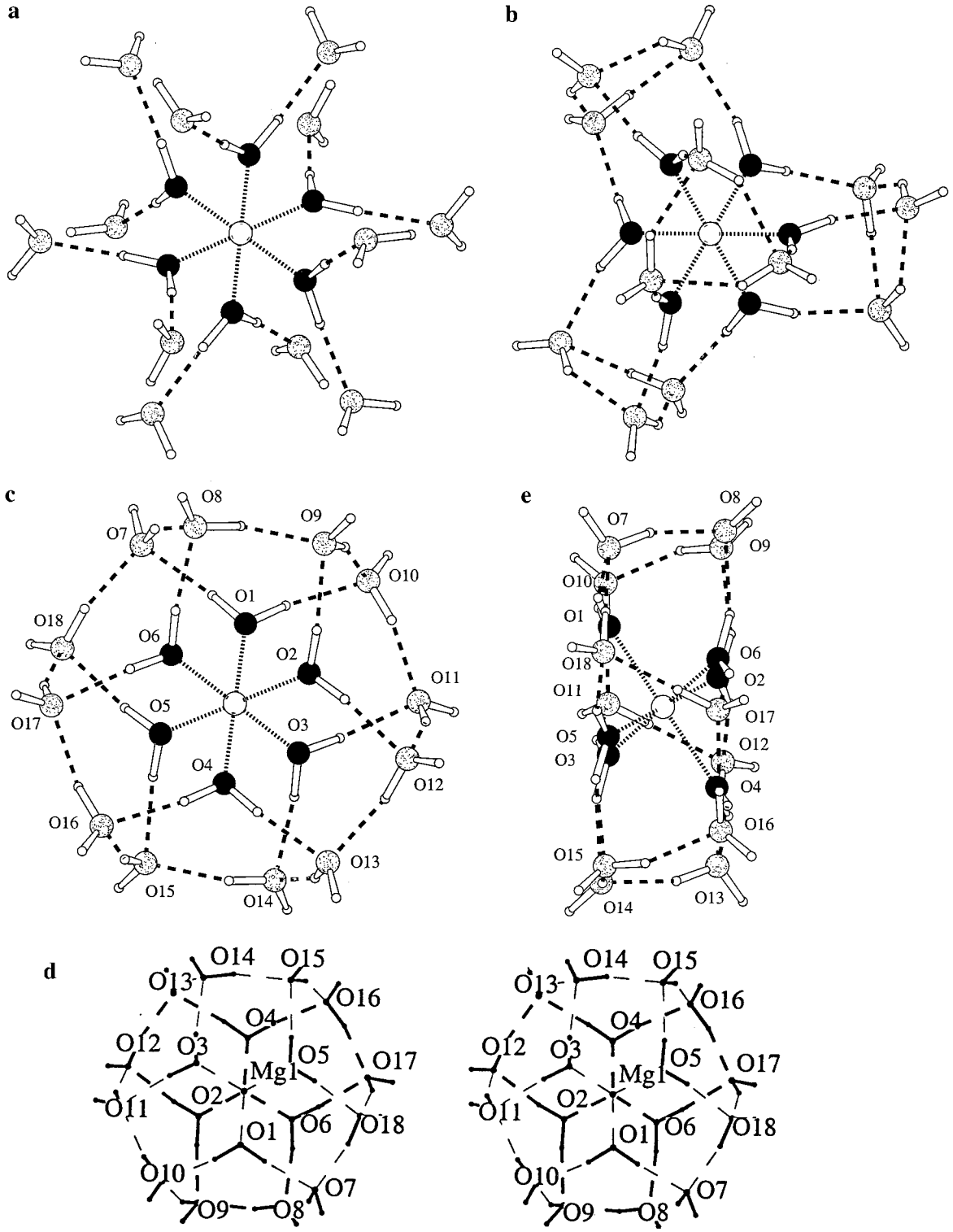

Figure 3. Optimized structures of various models of the $Mg[H_2O]_6^{2+}\cdot[H_2O]_{12}$ complex. (a) The PSS conformer obtained from a BP/DN** reoptimization of the structure reported by Pavlov et al.,[30] (b) the PCR conformer obtained from a B3LYP/6-31+G** reoptimization of the structure reported by Pye and Rudolph,[57] (c)−(e) two views of our S_6 model optimized at the B3LYP/6-31+G** computational level. The view in (d) is perpendicular to that in (c) and shows that the structure is somewhat flattened; (e) is a stereoview.

Aqueous solutions containing Mg^{2+} ions have also been studied using X-ray diffraction methods and Mg···O distances for second-shell water molecules have been reported in the range from 4.10 to 4.28 Å, some 0.2 Å less than the calculated values for the PSS conformer of $Mg[H_2O]_6^{2+}\cdot[H_2O]_{12}$,[80,83,84,86,87,180] but near the value we find for our model (vide infra). Molecular dynamics simulations of solutions containing divalent magnesium ions have found somewhat longer Mg···O distances, in the range from 4.30 to 4.47 Å.[65−67,80,84,181] Our analysis of the crystal structures in the CSD gave 4.31 Å; see Table 5. The O···O distance between first- and second-shell water molecules estimated by electron diffraction methods is 2.75−2.81 Å in these solutions, which is smaller than this distance in bulk water and slightly smaller than in the PSS complex.[80] The binding enthalpy for the PSS model of $Mg[H_2O]_6^{2+}\cdot[H_2O]_{12}$ is found to be 474, 516, and 480 kcal/mol at the BP/DN**, MP2(FULL)/

6-311++G(2d,2p), and B3LYP/6-311++G(2d,2p) computational levels using the BP/DN** optimized geometry (see Table 2); Pavlov et al.[30] reported a value of 461 kcal/mol.[30]

Pye and Rudolph[57] recently reported the results of Hartree−Fock optimizations for three different models of the $Mg[H_2O]_6^{2+}\cdot[H_2O]_{12}$ complex. Two of their models, which we will denote PRA and PRB, involve no hydrogen bonds between second-shell water molecules and both have T_h symmetry, the same as that found for the global minimum of the $Mg[H_2O]_6^{2+}$ complex. Model PRB is the symmetrized version of the structure reported by Pavlov et al.,[30] while model PRA has the second-shell water molecules rotated by 90°. Their frequency analyses clearly showed, however, that neither of these forms were local minima on the PES at the HF/6-31G*//HF/6-31G* computational level. We used their final Z-matrices for these complexes as input and reoptimized both structures at the BP/DN** level. At the B3LYP/6-311++G(2d,2p)//BP/DN** level the PRA and PRB models have nearly the same energy as the reoptimized PSS form; see Table 1S.

Desymmetrization along the highest frequency mode, which eliminates the T_h inversion center, led Pye and Rudolph[57] to a novel model for $Mg[H_2O]_6^{2+}\cdot[H_2O]_{12}$, which we label PRC, that has only T symmetry. They found this conformer to be some 34 kcal/mol lower in energy than the T_h forms at the HF/6-31G* level, and a frequency analysis at this level showed that it was a local minimum on the PES. For this conformer of $Mg[H_2O]_6^{2+}\cdot[H_2O]_{12}$, the $Mg[H_2O]_6^{2+}$ unit effectively interacts with four distinct (cyclic) water trimers. Using their Z-matrix as input, but maintaining only D_2 symmetry, we reoptimized this structure at the BP/DN**, B3LYP/6-31G*, B3LYP/6-31+G*, B3LYP/6-31+G**, and B3LYP/6-311++G** levels (see Figure 3b); frequency analyses at all these B3LYP computational levels confirm that a conformer with four water trimers hydrogen bonded to $Mg[H_2O]_6^{2+}$ is a local minimum on the PES, in agreement with the HF/6-31G* results.[57] The average Mg···O distance for the six inner-shell water molecules is about 2.10 Å at the various computational levels, about 0.01 Å shorter than the corresponding Mg−O distances in the $Mg[H_2O]_6^{2+}$ complex; see Table 4. The average Mg···O distance to the outer-shell water molecules in this conformer is some 0.2 Å *shorter* than that found for the PSS form (optimized at the BP/DN** level) and these shorter Mg···O distances are in much better agreement with the results of X-ray diffraction studies on the second hydration sphere of Mg^{2+} in solution, although the values are not directly comparable.[80] The average O···O distance in each of the water trimers in this complex is 2.807 Å, slightly *longer* than this distance for an isolated water trimer, 2.778 Å at the B3LYP/6-31+G** computational level (see Table 3S); the total molecular energy of one of the trimers at the geometry in this complex is only 1.2 kcal/mol *higher* than that for an isolated completely optimized (cyclic) trimer.

The hydrogen atoms from the second-shell water molecules of the PRC structure, unlike those in the PSS structure, fall into two groups: 12 "free" hydrogen atoms and 12 hydrogen atoms involved in hydrogen bonds within the second shell, 5.14 and 4.33 Å from the central magnesium ion, respectively, at the B3LYP/6-31+G** level. Figure 3b clearly shows that the dipoles of the outer-shell water molecules are *not* directed toward Mg^{2+} in the PRC form. We find the PRC form of $Mg[H_2O]_6^{2+}\cdot[H_2O]_{12}$ to be 23.8−32.0 kcal/mol *lower* in energy than the PSS form at various computational levels when the BP/DN** optimized geometries are employed for both structures. Calculated net binding enthalpies of the PRC conformer of $Mg[H_2O]_6^{2+}\cdot[H_2O]_{12}$ are given in Table 2 and, as might be expected with so many water molecules involved in this complex, there are relatively large differences among the values of the binding enthalpies calculated at different computational levels, e.g., using the 6-311++G** basis set, the MP2(FULL) value of ΔH°_{298} is greater than the B3LYP value by about 20 kcal/mol. Similar differences (although smaller in magnitude) were found for $Mg[H_2O]_6^{2+}\cdot[H_2O]$ (see above). In Table 6 we list enthalpy changes for the reaction

$$Mg[H_2O]_6^{2+}\cdot[H_2O]_{12} \rightarrow Mg[H_2O]_6^{2+} + 12H_2O \quad (3)$$

The net binding energy of the 12 second-shell water molecules is 166.1 kcal/mol at the B3LYP/6-311++G(3df,3pd)//B3LYP/6-311++G** computational level. The value of ΔH°_{298} for this reaction from MP2(FULL) calculations using the 6-311++G-(2d,2p) basis set (where all geometries were optimized at the BP/DN** level) is some 20 kcal/mol *higher* than the value of ΔH°_{298} from the corresponding B3LYP calculation. The net binding energy per trimer unit to the central $Mg[H_2O]_6^{2+}$ core is 31.2 kcal/mol at the B3LYP/6-311++G(3df,3pd)//B3LYP/6-311++G** level; see Table 6.

The NPA charge on the magnesium ion in the PRC structure is +1.77e at the B3LYP/6-31+G* computational level, indicating some transfer of electron density from the water ligands to the ion. (For comparison, we note that the charge on the magnesium ion in the $Mg[H_2O]_6^{2+}$ complex at this level is nearly the same, +1.78e.) Interestingly, the net charge on the $Mg[H_2O]_6^{2+}$ moiety in $Mg[H_2O]_6^{2+}\cdot[H_2O]_{12}$ is slightly less positive, +1.66e, showing an overall donation of electron density from the second-shell water molecules. The NPA charge on each of the oxygen atoms of the first-shell water molecules is more negative than the charge on the oxygen atoms of the water molecules in the second shell; the additional density residues primarily in the oxygen 2p orbitals of the inner-shell water molecules.

Despite the aesthetically appealing nature and relatively low energy of the PRC form of $Mg[H_2O]_6^{2+}\cdot[H_2O]_{12}$,[57] it seems unlikely that a structure with a hydrogen-bonded network comprised of four water trimers in the second shell that effectively do not interact with each other would be the global minimum on the PES.[120−134] We initiated a series of BP/DN** geometry optimizations of $Mg[H_2O]_6^{2+}\cdot[H_2O]_{12}$ to search for a structure with a more integrated hydrogen-bonded network surrounding Mg^{2+}; no symmetry constraints were employed during the optimizations. The lowest energy form we found from these calculations is some 15 kcal/mol *lower* in energy than that from our reoptimized PRC form at this computational level; single point MP2(FULL) and B3LYP calculations, using the BP/DN** geometries of these two forms, confirm that our structure is lower in energy; see Table 1S.

Two views of this new form of $Mg[H_2O]_6^{2+}\cdot[H_2O]_{12}$, which is identified as having S_6 symmetry in the software package Jaguar,[182] are shown in Figures 3c,d; a stereoview is shown in Figure 3e. Starting from the final BP/DN** geometry, we optimized this form of $Mg[H_2O]_6^{2+}\cdot[H_2O]_{12}$ at the B3LYP/6-31G*, B3LYP/6-31+G*, and B3LYP/6-31+G** computational levels. Structural details from the B3LYP/6-31+G** optimization are given in Figures 1S and Table 6S of the Supporting Information. Frequency analyses at all these levels confirm that this structure is a local minimum on the PES; the calculated frequencies of our structure are listed in Table 7S of the Supporting Information. We find this structure of $Mg[H_2O]_6^{2+}\cdot[H_2O]_{12}$ to be 10.3, 9.2, and 8.3 kcal/mol *lower* in energy than the PRC structure at the B3LYP/6-31G*//B3LYP/6-31G*, B3LYP/6-31+G*//B3LYP/6-31+G*, and B3LYP/6-31+G**//B3LYP/6-31+G** computational levels, respectively; see Table

TABLE 7: Second Hydration Shell around $Mg[H_2O]_6^{2+}$ at 3.2−4.7 Å from the Magnesium Ion[146−178]

(a) Atoms in the Second Hydration Shell of Mg^{2+} [a]

ANAPHS[146]	12O				8H	
AQMEDA[147]	12O			4C	8H	
BADTEX01[148]	10O	2N	2O		10H	
BADTEX10[148]	10O	2N	2O		8H	
CAWTID[150]	10O		2O	4C	4H	
CIRVAA[151]	12O			4C	4H	
CIRVAA01[152]	12O			4C	4H	
FEDQUA[154]	12O		2O	2C	14H	
FEDQUA01[155]	12O		2O	2C	14H	
GATLUI[156]	10O		4O		12H	
GIJVEA[175]	8N			2N	12H	
GOLPIG[158]	10O			2C	12H	
GOLPIG[158]	10O			2C	14H	
GUHHOG[159]	12O			4C	12H	
HAHWAO[160]	12O		2O	2C	14H	
HETZUB[161]	12O		4O	2C	16H	
HMTMGC10[162]	4O	7N		2C	12H	
KEQRAZ[163]	12O		4O	6C	12H	
KIMNID[164]	12O		2N	4C	16H	
MGCITD[165]	12O			6C	10H	
MGEDTA01[166]	12O			2C	18H	
MGNTSP[167]	10O	2N	2O	4C	6H	
RATRIN[168]	12O				10H	
RIVCAA[169]	6O	6N	2O	2N	5C	8H
SIMZUJ[170]	12O		2O	4C	12H	
VOPCEI[174]	12O		2O	2N	2C	8H
VUKMIX[175]	12O				8H	
WIKXAP[176]	12O		2O	2C	12H	
WIKXAP[176]	10O			2C	12H	
ZARMEK[177]	11O		3O	1N		8H
fluoride, chloride, bromide, sulfur						
BIKPUG[149]	4O	2N	4Br			10H
DXMGHC10[153]	4O	2Cl			2C	12H
TEKBIU[171]	10O			2S	2C	10H
THIAMG10[172]	6O	4Cl			4C	14H
TOXDMG[173]	4O	2Cl				10H
ZURWIS[178]	10O	2N		2O	2F	8H

(B) Analysis of Number of Atoms in the Second Hydration Shell in Crystal Structures[b]

	A	B	C	D	E
ANAPHS	12	0	8	20	12
AQMEDA	12	4	8	24	16
BADTEX01	12	2	10	24	14
BADTEX10	12	2	8	22	14
CAWTID	10	6	4	20	16
CIRVAA	12	4	4	20	16
CIRVAA01	12	4	4	20	16
FEDQUA	12	4	14	30	16
FEDQUA01	12	4	14	30	16
GATLUI	10	4	12	26	14
GIJVEA	8	2	12	22	10
GOLPIG	10	2	12	24	12
GOLPIG	10	2	14	26	12
GUHHOG	12	4	12	28	16
HAHWAO	12	4	14	30	16
HETZUB	12	6	16	34	18
HMTMGC10	11	2	12	25	13
KEQRAZ	12	10	12	34	22
KIMNID	12	6	16	34	18
MGCITD	12	6	10	28	18
MGEDTA01	12	2	18	32	14
MGNTSP	10	6	6	22	16
RATRIN	12	5	10	27	17
RIVCAA	12	8	8	28	20
SIMZUJ	12	4	12	28	16
VOPCEI	12	4	8	24	16
VUKMIX	12	2	8	22	14
WIKXAP	12	4	12	28	16
WIKXAP	10	0	12	22	10
ZARMEK	11	4	8	23	15
av				25.9	15.3
fluoride, chloride, bromide, sulfur					
BIKPUG	10	0	10	20	10
DXMGHC10	6	2	12	20	8
TEKBIU	10	4	10	24	14
THIAMG10	10	4	14	28	14
TOXDMG	6	0	10	16	6
ZURWIS	12	4	8	24	16
total av				25.2	14.6

[a] Oxygen, nitrogen, carbon, and hydrogen only. Left of the vertical line are atoms hydrogen bonded to the six water molecules in the inner shell. Right of the vertical line are other atoms in the second shell (defined by the distance to Mg^{2+}). [b] Oxygen, nitrogen, carbon, hydrogen only. Key to the columns in (b): A, number of atoms hydrogen bonded to inner $Mg[H_2O]_6^{2+}$; B, number of non-H atoms in addition; C, number of hydrogen atoms; D, total number of atoms in this distance range (3.2−4.7 Å) (cols 1−3); E, total number of non-H atoms in this distance range (3.2−4.7 Å) (cols 1 and 2).

1S. It is evident from Figure 3c that the main structural units of the water molecules in this model of $Mg[H_2O]_6^{2+}\cdot[H_2O]_{12}$ are (cyclic) pentamers constructed from four second-shell water molecules and one first-shell water molecule. It should be noted, however, that the structure of these pentamers is somewhat different from the structure of the global minimum on the PES of cyclic $[H_2O]_5$, in which one hydrogen atom from each water molecule is *not* involved in a hydrogen bond.[183] For the pentamers in our form of $Mg[H_2O]_6^{2+}\cdot[H_2O]_{12}$, both hydrogen atoms from the inner-shell water molecule are hydrogen-bonded in the same pentagonal ring. Furthermore, neither of the hydrogen atoms from one of the four water molecules in the second shell is hydrogen-bonded in that ring; see Figure 3c. (The energy difference between a pentamer at its geometry in $Mg[H_2O]_6^{2+}\cdot[H_2O]_{12}$ and a fully optimized cyclic water pentamer is substantial, 19.2 kcal/mol at the B3LYP/6-31+G** level.) It is clear from Figure 3d that our model of $Mg[H_2O]_6^{2+}\cdot[H_2O]_{12}$ has a "sandwich-like" structure, similar to that found by Glendening et al.[14] and Kim et al.[21] for the inner-shell water molecules of $Na[H_2O]_6^{2+}$, where the cation−water interactions are relatively weak.

The new structure that we present here for $Mg[H_2O]_6^{2+}\cdot[H_2O]_{12}$ can be viewed as the result of inserting an $Mg[H_2O]_6^{2+}$ octahedron inside a regular dodecahedron (with a distance of 2.7−2.8 Å between vertexes); see Figure 4. Twelve of the vertexes are locations at which hydrogen bonds from the six inner-shell water molecules would lie. The pentagonal dodecahedron is a common motif for water in clathrate compounds such as chlorine hydrate ($8\ Cl_2\cdot 46H_2O$).[184−187] The six inner-shell water molecules in this new model of $Mg[H_2O]_6^{2+}\cdot[H_2O]_{12}$ remain in an essentially octahedral arrangement; each Mg^{2+}-OH_2 unit is planar to within ±1°. This is rather interesting because in their MD simulation of hydrated Mg^{2+}, Martinez et al.[45] found a tilt angle of 15°. A neutron diffraction study of hexa-aquo magnesium bis (hydrogen maleate) also shows tilt angles of the order of 10° (10.5°, 5.9°, 10.3° with esd values of the order of 0.5°).[152] Such distortions in the crystalline state depend on the locations of atoms to which hydrogen bonding occurs, but these deviations from coplanarity of the water molecule and the $Mg^{2+}\cdots O$ vector are very small; values for tilt angles would need to be as high as 70° (180−109.5°) if additional hydrogen bonding to an inner-sphere water molecule were to occur.

The average O−H distance for the six inner-shell water molecules is 0.976 Å, only slightly longer than the O−H distance in an isolated $Mg[H_2O]_6^{2+}$ complex, 0.970 Å. The free O−H bond lengths for the second-shell water molecules are all nearly 0.968 Å. The average Mg−O distance for the inner-shell water molecules in this form of $Mg[H_2O]_6^{2+}\cdot[H_2O]_{12}$ is 2.098 Å at the B3LYP/6-31+G** level. (For comparison, we note

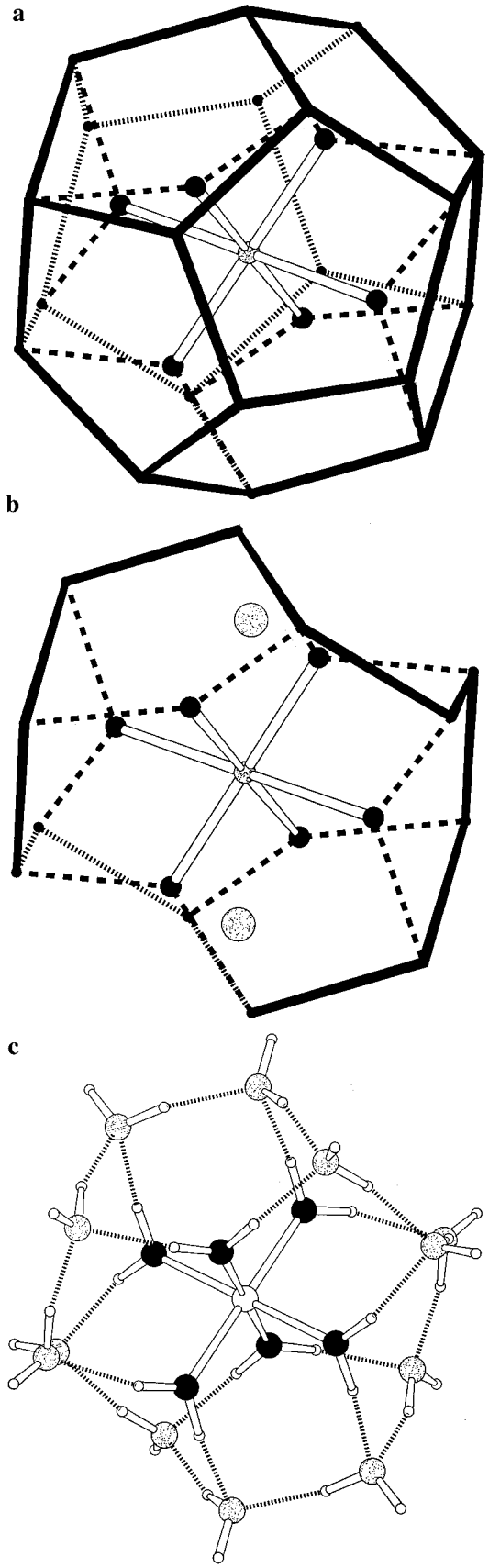

Figure 4. (a) Diagram of a pentagonal dodecahedron with an octahedron inserted within it. Possible interactions (as in our model complex) are indicated by dashed lines. The far side of the dodecahedron is indicated by broken lines. (b) View in (a) with short interactions removed. Two non-hydrogen-bonded vertexes are shown as speckled balls. (c) View of our model in the same orientation as the dodecahedron in (a) and (b).

that the average Mg−O distances for PRC form of $Mg[H_2O]_6^{2+}\cdot[H_2O]_{12}$ and for $Mg[H_2O]_6^{2+}$ itself are 2.101 and 2.111 Å, respectively, at this computational level.)

The average Mg···O distances to the outer-shell water molecules is 4.130 Å, which is significantly smaller than this distance for the PRC structure, 4.283 Å; experimental values are in the range 4.10−4.28 Å.[80] The average distance between oxygen atoms in the first and second shells for our structure is 2.810 Å, which is in reasonable agreement with the observed range of values for this parameter, 2.75−2.81 Å.[80] The average distance from the magnesium ion to the 12 free second-shell hydrogen atoms is 5.02 Å, while the distance to the 12 hydrogen atoms involved in hydrogen bonds is only 4.09 Å at the B3LYP/6-31+G** level. These values are slightly smaller than the corresponding values for the PRC structure, as a result of the more integrated hydrogen-bonding network. It should be noted, however, that no splitting of the second peak of the Mg−H radial distribution function is observed in molecular dynamics studies in solution.[11] This difference may be a consequence of the isolated nature of our cluster.

The NPA charges on the atoms in our form of $Mg[H_2O]_6^{2+}\cdot[H_2O]_{12}$ are very similar to those in the PRC form. The charge on the magnesium ion is +1.77e, the net charge on the $Mg[H_2O]_6^{2+}$ moiety is +1.66e, and the oxygen atoms of the inner-shell water molecules are more negatively charged than those of the outer-shell water molecules at the B3LYP/6-31+G** level.

Calculated values for the infrared Mg−O breathing mode for a variety of divalent magnesium complexes are given in Table 8S. This frequency decreases for $Mg[H_2O]_6^{2+}$ as n increases from 1 to 6. Including only one water molecule in the second shell, however, already reverses this trend and υ_{Mg-O} increases a few cm^{-1}. Including 12 water molecules in the second shell increases this frequency to about 340 cm^{-1} at the B3LYP/6-31+G**//B3LYP/6-31+G** computational level for both our form and the PRC form; Pye and Rudolph[57] report a value of 356 cm^{-1} from the HF/6-31G* frequency analysis. Using larger basis sets and including the effects of electron correlation reduce the calculated frequency by some 15 cm^{-1}; see Table 8S. The experimental value of this mode (in O_h symmetry) is 356 cm^{-1}.[57]

Concluding Remarks

The present MP2(FULL) and B3LYP calculations substantiate the premise that in the presence of six or fewer water molecules, Mg^{2+} prefers to bind all of them into its first coordination sphere, rather than partitioning them into two coordination spheres. This is also evident in the crystal structures of hydrated magnesium salts, in which $Mg[H_2O]_6^{2+}$ units abound. This hexahydrate optimizes the transfer of charges from the water ligands to the magnesium ion. Comparing the total molecular energies of $Mg[H_2O]_5^{2+}$ and $Mg[H_2O]_4^{2+}\cdot[H_2O]$, or of $Mg[H_2O]_6^{2+}$, $Mg[H_2O]_5^{2+}\cdot[H_2O]$, and $Mg[H_2O]_4^{2+}\cdot[H_2O]_2$ in our calculations, however, it is evident that for a given number of water molecules MP2(FULL) calculations generally find a significantly greater energy separation between the complex with all the water molecules in the first shell and those complexes with the water molecules distributed between the first and second shells. B3LYP and MP2(FULL) calculations using the 6-311++G** basis set both find that the conversion $Mg[H_2O]_5^{2+} \rightarrow Mg[H_2O]_4^{2+}\cdot[H_2O]$ is entropically unfavored. On the other hand, the conversions $Mg[H_2O]_6^{2+} \rightarrow Mg[H_2O]_5^{2+}\cdot[H_2O]$ and $Mg[H_2O]_6^{2+} \rightarrow Mg[H_2O]_4^{2+}\cdot[H_2O]_2$ are entropically favored at the B3LYP/6-311++G** level. In comparing the calculated geometrical parameters from the two methods for the same complex, we also find some differences. For example with a given basis

set, B3LYP calculations on the monohydrate $Mg[H_2O]^{2+}$ find shorter Mg−O distances, greater charge transfer and larger binding enthalpies than do the corresponding MP2(FULL) calculations, whereas for the hexahydrate $Mg[H_2O]_6^{2+}$, B3LYP calculations find longer Mg−O distances, smaller charge transfer and smaller binding enthalpies than do the corresponding MP2-(FULL) calculations.

The second coordination shell, which forms in the presence of at least seven waters, is filled in our model by 12 water molecules. This is the number expected to interact by hydrogen bonding to the inner six water molecules: two hydrogen bonds between second-sphere water molecules and each inner-sphere water. The second-sphere water molecules are presumed to bind through a mix of electrostatic interactions with the Mg^{2+} and hydrogen bonding interactions to the first-shell water molecules and to other second-shell water molecules. When there is only a single water molecule in the second shell, MP2(FULL) and B3LYP optimizations are in agreement that the lowest-energy form of $Mg[H_2O]_6^{2+}\cdot[H_2O]$ has the second-shell water molecule hydrogen-bonded to two different water molecules in the first shell (Mg···O = 3.93 Å); the form of this complex in which the second-shell water molecule is hydrogen bonded to one first-shell water molecule (Mg···O = 4.26 Å), however, is only about 1 kcal/mol higher in energy. The dipole moment of the second-shell water molecule (in either form of $Mg[H_2O]_6^{2+}\cdot[H_2O]$) is oriented in a direction toward the central magnesium ion; the dipole moments of the six inner-shell water molecules are directed similarly.

When there are 12 water molecules in the second shell, however, intricate hydrogen-bonding networks are possible that can help stabilize the complex. Our calculations, in accord with those of Pye and Rudolph,[57] suggest that the dipolar interactions between the 12 second-shell water molecules and the (screened) divalent magnesium ion (Mg···O > 4.1 Å) in $Mg[H_2O]_6^{2+}\cdot[H_2O]_{12}$ are *not* sufficiently strong to orient the dipole moments of these second-sphere water molecules in a direction toward the central magnesium dication. This finding focuses attention on the structure of the hydrogen-bonding network in searching for the global minimum on the PES of the $Mg[H_2O]_6^{2+}\cdot[H_2O]_{12}$ complex. Pye and Rudolph[57] discovered the first true local minimum (on the HF/6-31G* PES) of this complex, and our higher level calculations at B3LYP/6-31G*, B3LYP/6-31+G*, B3LYP/6-31+G** and B3LYP/6-311++G** levels confirm that their structure is a local minimum on these PESs. Their (PRC) structure has *T* symmetry and the 12 second-sphere water molecules are grouped into four water trimers attached to an inner octahedral $Mg[H_2O]_6^{2+}$ moiety (Figure 3b).

We have now identified a second local minimum on the B3LYP/6-31G*, B3LYP/6-31+G* and B3LYP/6-31+G** PESs of $Mg[H_2O]_6^{2+}\cdot[H_2O]_{12}$. This new minimum, which has only S_6 symmetry, has a more integrated hydrogen-bonded network than the structure proposed by Pye and Rudolph[57] and it is calculated to be some 8−10 kcal/mol *lower* in energy at a variety of computational levels. The presence of a second solvation sphere surrounding Mg^{2+} has relatively little effect on the net charge on the magnesium ion compared to that in $Mg[H_2O]_6^{2+}$ (+1.78e), whether the PRC form (+1.77e) or our form (+1.77e) of the hydrogen-bonded network is used for the calculation. The main effect of the second hydration sphere is to change the net charge on the first hydration sphere from about +0.22 to −0.12. We cannot, of course, claim from these calculations that our new structure is the global minimum on the PES, but it is currently the lowest-energy form that is known. The geometry of the hydrogen-bonded network in our S_6 structure

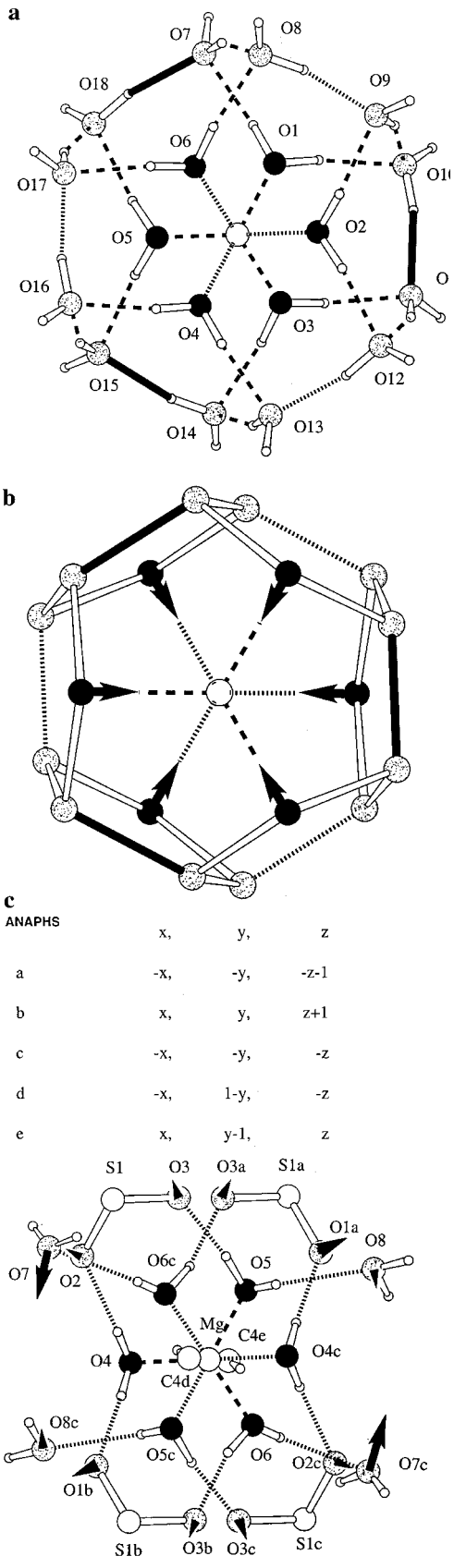

Figure 5. (a) Our new model of $Mg[H_2O]_6^{2+}\cdot[H_2O]_{12}$. View down the 3-fold axis. Uppermost hydrogen bonds are represented by filled bonds. (b) Pentagonal dodecahedron with a contained octahedron drawn in the same orientation as (a). Arrows indicate necessary movements to give the structure in (a). (c) Crystal structure of ANAPHS in the same orientation as (a) and (b). Arrows indicate the distance to the model in (a). Symmetry codes a−e are included.

contains pentameric clusters comprised of four water molecules from the second shell and one from the first shell. Water pentamers[184−187] have been found in many hydrate crystal structures and are thought to be common in pure water. Thus the second hydration sphere appears to provide a smooth transition between the ligation sphere of Mg^{2+} and bulk solvent.

A comparison of our model structure of $Mg[H_2O]_6^{2+}\cdot[H_2O]_{12}$ (Figure 5a) with a regular dodecahedron of water molecules (Figure 5b) shows that the two structures are remarkably similar. The main difference is that six of the water molecules of the dodecahedron lie in the first, rather than second coordination shell of water molecules (see heavy black arrows). This leaves sites for the binding of water at 14 out of the 20 vertexes of the water dodecahedron in the second shell. But only 12 of these 14 are hydrogen bonded to the six water molecules of the inner coordination shell. Two positions (13th and 14th coordination positions) are left unoccupied. As a result the model is not spherically symmetric but somewhat flat (as seen in Figure 3d). Presumably the locations of these 13th and 14th coordination positions vary dynamically. In crystal structures they are generally filled with ligands. An example (ANAPHS)[146] is given in Figure 5c where two hydrocarbon groups (C−H) fill the two axial positions in the center of the diagram. Thus we suggest that two additional (13th and 14th) positions on the $Mg[H_2O]_6^{2+}\cdot[H_2O]_{12}$ complex are available to bind water or ligand molecules, leading to a coordination number of 14 in the second hydration shell. These two ligands are, however, differently bonded and more weakly held than the other 12 ligands.

Experimental data have suggested, as noted earlier, that the second coordination shell of magnesium holds 12 water molecules.[80,83,84,86,87] Simple geometric considerations suggest that the second shell (radius about 4.3 Å; see Table 5) has about 4 times the surface area of the first sphere (radius about 2.06 Å; see Table 5). Since the latter holds six water molecules, a maximum of 24 in the second sphere is implied. Crystal structures (see Table 7S) also suggest that this value may be higher than 12 and a value of 13 has been deduced from a molecular dynamics simulation.[45] But those groups that pack in the second coordination shell (in addition to the 12 that are hydrogen bonded directly to the six water molecules of the first coordination sphere) are comparatively weakly held and therefore may be lost more readily. The good metric fit of the $Mg(H_2O)_6^{2+}$ orientation within a $(H_2O)_{14}$ polyhedron may explain the high affinity of the naked magnesium ion for water since this structure will cause a minimal distortion to bulk water.

Acknowledgment. This work was supported by National Institutes of Health grants GM31186, CA10925, CA06927, and also supported by an appropriation from the Commonwealth of Pennsylvania. We thank the Advanced Scientific Computing Laboratory, NCI-FCRF, for providing time on the Cray YMP and J90 computers. We also thank Dr. Maria Pavlov and Dr. Cory Pye for providing coordinates for their structures of $Mg[H_2O]_6^{2+}\cdot[H_2O]_{12}$. The contents of this manuscript are solely the responsibility of the authors and do not necessarily represent the official views of the National Cancer Institute, or any other sponsoring organization.

Supporting Information Available: Table 1S, total molecular energies (a.u.) of various divalent magnesium hydrates. Table 2S. thermal corrections to 298 K, S (a.u.), entropies, S (cal/(mol K)), and heat capacities, C_V (cal/(mol K)), calculated at the B3LYP/6-311++G**//B3LYP/6-311++G** computational level. Table 3S, calculated geometrical parameters for the water dimer and (cyclic) water trimer. Table 4S, calculated binding enthalpies, ΔH°_{298} (kcal/mol), of the water dimer and trimer (cyclic). Table 5S, unscaled calculated frequencies, ν (cm^{-1}), and IR intensities, I (kM/mol), of $Mg[H_2O]_6^{2+}$. Table 6S, selected Mg−O and Mg−H (Å) distances for our form of $Mg[H_2O]_6^{2+}\cdot[H_2O]_{12}$ obtained from the B3LYP/6-31+G** optimization. Table 7S, unscaled calculated frequencies, ν (cm^{-1}), and IR intensities, I (kM/mol) of our form of $Mg[H_2O]_6^{2+}\cdot[H_2O]_{12}$ obtained at the B3LYP/6-31+G** computational level. Table 8S, calculated Mg−O infrared breathing frequencies (cm^{-1}). Figure 1Sa−c, model of $Mg[H_2O]_6^{2+}\cdot[H_2O]_{12}$. This material is available free of charge via the Internet at http://pubs.acs.org.

References and Notes

(1) Kebarle, P. *Modern Aspects of Electrochemistry*; Plenum Press: New York, 1974; Vol. 9.
(2) Marcus, Y. *Ion Solvation*; Wiley-Interscience: Chichester, U.K., 1985; Vol. 2.
(3) Searles, S. K.; Kebarle, P. *J. Phys. Chem.* **1968**, *72*, 742−743.
(4) Dzidic, I.; Kebarle, P. *J. Phys. Chem.* **1970**, *74*, 1466−1474.
(5) Kebarle, P. *Annu. Rev. Phys. Chem.* **1977**, *28*, 445−476.
(6) Holland, P. M.; Castleman, A. W. *J. Am. Chem. Soc.* **1980**, *102*, 6174−6175.
(7) Holland, P. M.; Castleman, A. W. *J. Chem. Phys.* **1982**, *76*, 4195−4205.
(8) Burnier, R. C.; Carlin, T. J.; Reents, W. D.; Cody, R. B.; Lengel, R. K.; Freiser, B. S. *J. Am. Chem. Soc.* **1979**, *101*, 7127−7129.
(9) Magnera, T. F.; David, D. E.; Michl, J. *J. Am. Chem. Soc.* **1989**, *111*, 4100−4101.
(10) Magnera, T. F.; David, D. E.; Stulik, D.; Orth, R. G.; Jonkman, H. T.; Michl, J. *J. Am. Chem. Soc.* **1989**, *111*, 5036−5043.
(11) Marinelli, P. J.; Squires, R. R. *J. Am. Chem. Soc.* **1989**, *111*, 4101−4103.
(12) Dalleska, N. F.; Honma, K.; Sunderlin, L. S.; Armentrout, P. B. *J. Am. Chem. Soc.* **1994**, *116*, 3519−3528.
(13) Steel, E. A.; Merz, K. M.; Selinger, A.; Castleman, A. W. *J. Phys. Chem.* **1995**, *99*, 7829−7836.
(14) Glendening, E. D.; Feller, D. *J. Phys. Chem.* **1995**, *99*, 3060−3067.
(15) Feller, D.; Glendening, E. D.; Kendall, R. A.; Peterson, K. A. *J. Chem. Phys.* **1994**, *100*, 4981−4997.
(16) Rosi, M.; Bauschlicher, C. W. *J. Chem. Phys.* **1989**, *90*, 7264−7272.
(17) Kraemer, W. P.; Diercksen, G. H. F. *Chem. Phys. Lett.* **1970**, *5*, 463−465.
(18) Diercksen, G. H. F.; Kraemer, W. P. *Theor. Chim. Acta* **1972**, *387−392*.
(19) Kistenmacher, H.; Popkie, H.; E. C. *J. Chem. Phys.* **1973**, *59*, 5842−5848.
(20) Lee, H. M.; Kim, J.; Lee, S.; Mhin, B. J.; Kim, K. S. *J. Chem. Phys.* **1999**, 3995−4004.
(21) Kim, J.; Lee, S.; Cho, S. J.; Mhin, B. J.; Kim, K. S. *J. Chem. Phys.* **1995**, 839−849.
(22) Tongraar, A.; Liedl, K. R.; Rode, B. M. *J. Phys. Chem. A* **1998**, *102*, 10340−10347.
(23) Pye, C. C.; Rudolph, W. W.; Poirier, R. A. *J. Phys. Chem.* **1996**, *100*, 601−605.
(24) Pye, C. C. *J. Quantum Chem.* **2000**, *76*, 62−76.
(25) Tongraar, A.; Liedl, K. R.; Rode, B. M. *Chem. Phys. Lett.* **1998**, *286*, 56−64.
(26) Chandrasekhar, J.; Spellmeyer, D. C.; Jorgensen, W. L. *J. Am. Chem. Soc.* **1984**, *106*, 903−910.
(27) Topol, I. A.; Tawa, G. J.; Burt, S. K.; Rashin, A. A. *J. Chem. Phys.* **1999**, *111*, 10998−11014.
(28) Spears, K. G.; Fehsenfeld, F. C. *J. Chem. Phys.* **1972**, *56*, 5698−5705.
(29) Walker, N. R.; Dobson, M. P.; Wright, R. R.; Barran, P. E.; Murrell, J. N.; Stace, A. J. *J. Am. Chem. Soc.* **2000**, *122*, 11138−11145.
(30) Pavlov, M.; Siegbahn, P. E. M.; Sandstrom, M. *J. Phys. Chem. A* **1998**, *102*, 219−228.
(31) Dudev, T.; Lim, C. *J. Phys. Chem. A* **1999**, *103*, 8093−8100.
(32) Klobukowski, M. *Can. J. Chem.−Rev. Can. Chim.* **1992**, *70*, 589−595.
(33) Bauschlicher, C. W.; Sodupe, M.; Partridge, H. *J. Chem. Phys.* **1992**, *96*, 4453−4463.
(34) Bock, C. W.; Katz, A. K.; Glusker, J. P. *J. Am. Chem. Soc.* **1995**, *117*, 3754−3763.
(35) Katz, A. K.; Glusker, J. P.; Beebe, S. A.; Bock, C. W. *J. Am. Chem. Soc.* **1996**, *118*, 5752−5763.

(36) Carugo, O.; Djinovic, K.; Rizzi, M. *J. Chem. Soc.-Dalton Trans.* **1993**, 2127−2135.
(37) Bock, C. W.; Glusker, J. P. *Inorg. Chem.* **1993**, *32*, 1242−1250.
(38) Bock, C. W.; Kaufman, A.; Glusker, J. P. *Inorg. Chem.* **1994**, *33*, 419−427.
(39) Markham, G. D.; Glusker, J. P.; Bock, C. L.; Trachtman, M.; Bock, C. W. *J. Phys. Chem.* **1996**, *100*, 3488−3497.
(40) Bock, C. W.; Katz, A. K.; Markham, G. D.; Glusker, J. P. *J. Am. Chem. Soc.* **1999**, *121*, 7360−7372.
(41) Trachtman, M.; Markham, G. D.; Glusker, J. P.; George, P.; Bock, C. W. *Inorg. Chem.* **1998**, *37*, 4421−4431.
(42) Katz, A. K.; Glusker, J. P.; Markham, G. D.; Bock, C. W. *J. Phys. Chem. B* **1998**, *102*, 6342−6350.
(43) Sanchez-Marcos, E.; Pappalardo, R. R.; Rinaldi, D. *J. Phys. Chem.* **1991**, *95*, 8928−8932.
(44) Pappalardo, R. R.; Marcos, E. S. *J. Phys. Chem.* **1993**, *97*, 4500−4504.
(45) Martinez, J. M.; Pappalardo, R. R.; Marcos, E. S. *J. Am. Chem. Soc.* **1999**, *121*, 3175−3184.
(46) Akesson, R.; Pettersson, L. G. M.; Sandstrom, M.; Wahlgren, U. *J. Am. Chem. Soc.* **1994**, *116*, 8691−8704.
(47) Rotzinger, F. P. *J. Am. Chem. Soc.* **1996**, *118*, 6760−6766.
(48) Lee, S.; Kim, J.; Park, J. K.; Kim, K. S. *J. Phys. Chem.* **1996**, *100*, 14329−14338.
(49) Rudolph, W. W.; Pye, C. C. *Phys. Chem. Chem. Phys.* **1999**, *1*, 4583−4593.
(50) Rudolph, W. W.; Pye, C. C. *J. Phys. Chem. B* **1998**, *102*, 3564−3573.
(51) Chang, C. M.; Wang, M. K. *Chem. Phys. Lett.* **1998**, *286*, 46−50.
(52) Bertini, I.; Luchinat, C.; Rosi, M.; Sgamellotti, A.; Tarantelli, F. *J. Inorg. Chem.* **1990**, *29*, 1460−1463.
(53) Hashimoto, K.; Yoda, N.; Iwata, S. *Chem. Phys.* **1987**, *116*, 193−202.
(54) Hartmann, M.; Clark, T.; vanEldik, R. *J. Am. Chem. Soc.* **1997**, *119*, 7843−7850.
(55) Lee, M. A.; Winter, N. W.; Casey, W. H. *J. Phys. Chem.* **1994**, *98*, 8641−8647.
(56) Hartmann, M.; Clark, T.; vanEldik, R. *J. Mol. Model* **1996**, *2*, 354−357.
(57) Pye, C. C.; Rudolph, W. W. *J. Phys. Chem. A* **1998**, *102*, 9933−9943.
(58) Bernal-Uruchurtu, M. I.; Ortega-Blake, I. *J. Chem. Phys.* **1995**, *103*, 1588−1598.
(59) Ortega-Blake, I.; Novaro, O.; Les, A.; Rybak, S. *J. Chem. Phys.* **1982**, *76*, 5405−5413.
(60) Rotzinger, F. P. *J. Am. Chem. Soc.* **1997**, *119*, 5230−5238.
(61) Floris, F.; Persico, M.; Tani, A.; Tomasi, J. *J. Chem. Phys.* **1995**, *195*, 207−220.
(62) Frenking, G.; Pidun, U. *J. Chem. Soc., Dalton Trans.* **1997**, 1653−1662.
(63) Duclev, T.; Lim, C. *J. Am. Chem. Soc.* **2000**, *122*, 11146−11153.
(64) Tongraar, A.; Liedl, K. R.; Rode, B. M. *J. Phys. Chem. A* **1997**, *101*, 6299−6309.
(65) Marx, D.; Fois, E.; Parrinello, M. *Int. J. Quantum. Chem.* **1996**, *57*, 655−662.
(66) Marx, D.; Sprik, M.; Parrinello, M. *Chem. Phys. Lett.* **1997**, *273*, 360−366.
(67) Marx, D.; Hutter, J.; Parrinello, M. *Chem. Phys. Lett.* **1995**, *241*, 457−462.
(68) Yamashita, M.; Fenn, J. B. *J. Phys. Chem.* **1984**, *88*, 4451−4459.
(69) Whitehouse, C. M.; Dreyer, R. N.; Yamashita, M.; Fenn, J. B. *Anal. Chem.* **1985**, *57*, 675−679.
(70) Jayaweera, P.; Blades, A. T.; Ikonomou, M. G.; Kebarle, P. *J. Am. Chem. Soc.* **1990**, *112*, 2452−2454.
(71) Blades, A. T.; Jayaweera, P.; Ikonomou, M. G.; Kebarle, P. *Int. J. Mass Spectrom. Ion Processes* **1990**, *102*, 251−267.
(72) Blades, A. T.; Jayaweera, P.; Ikonomou, M. G.; Kebarle, P. *J. Chem. Phys.* **1990**, *92*, 5900−5906.
(73) Peschke, M.; Blades, A. T.; Kebarle, P. *J. Phys. Chem. A* **1998**, *102*, 9978−9985.
(74) Rodriguez-Cruz, S. E.; Jockusch, R. A.; Williams, E. R. *J. Am. Chem. Soc.* **1999**, *121*, 1986−1987.
(75) Rodriguez-Cruz, S. E.; Jockusch, R. A.; Williams, E. R. *Soc. J. Am. Chem.* **1998**, *120*, 5842−5843.
(76) Stace, A. J.; Walker, N. R.; Firth, S. *J. Am. Chem. Soc.* **1997**, *119*, 10239−10240.
(77) Dobson, M. P.; Stace, A. J. *J. Chem. Soc., Chem. Commun.* **1996**, 1533−1534.
(78) Woodward, C. A.; Dobson, M. P.; Stace, A. J. *J. Phys. Chem.* **1996**, *100*, 5605−5607.
(79) Stace, A. *Science* **2001**, *294*, 1292−1293.
(80) Ohtaki, H.; Radnai, T. *Chem. Rev.* **1993**, *93*, 1157−1204.
(81) Albright, J. N. *J. Chem. Phys.* **1972**, *56*, 3783−3786.
(82) Caminiti, R.; Licheri, G.; Paschina, G.; Piccaluga, G.; Pinna, G. *Z. Naturforsch.* **1980**, *35*, 1361−1367.
(83) Caminiti, R.; Licheri, G.; Piccaluga, G.; Pinna, G. *J. Appl. Crystallogr.* **1979**, *12*, 34−38.
(84) Palinkas, G.; Radnai, T.; Dietz, W.; Szaaz, G.; Heinzinger, K. Z. *Naturforsch* **1982**, *A37*, 1049−1060.
(85) Bock, C. Unpublished results.
(86) Caminiti, R.; Cerioni, G.; Crisponi, G.; Cucca, P. *Z. Naturforsch.* **1988**, *A43*, 317−325.
(87) Caminiti, R. *Chem. Phys. Lett.* **1982**, *88*, 103−108.
(88) Allen, F. H.; Bellard, S.; Brice, M. D.; Cartwright, B. A.; Doubleday: A.; Higgs, H.; Hummelink, T.; Hummelink-Peters, B. G.; Kennard, O.; Motherwell, W. D. S.; Rodgers, J. R.; Watson, D. G. *Acta Crystallogr.* **1979**, *B35*, 2331−2339.
(89) Spartan, Version 5.0. Wavefunction Inc., Irvine, CA.
(90) Perdew, J. P. *Phys. Rev. A* **1986**, *33*, 8822−8824.
(91) Becke, A. D. *Phys. Rev. A* **1988**, *38*, 3098−3100.
(92) Frisch, M. J.; Trucks, G. W.; Schlegel, H. B.; Gill, P. M. W.; Johnson, B. G.; Robb, M. A.; Cheeseman, J. R.; Keith, T.; Petersson, G. A.; Montgomery, J. A.; Raghavachari, K.; Al-Laham, M. A.; Zakrzewski, V. G.; Ortiz, J. V.; Foresman, J. B.; Cioslowski, J.; Stefanov, B. B.; Nanayakkara, A.; Challacombe, M.; Peng, C. Y.; Ayala, P. Y.; Chen, W.; Wong, M. W.; Andres, J. L.; Replogle, E. S.; Gomperts, R.; Martin, R. L.; Fox, D. J.; Binkley, J. S.; Defrees, D. J.; Baker, J.; Stewart, J. J. P.; Head-Gordon, M.; Pople, J. A. *Gaussian94*, Revision A.1; Gaussian Inc.: Pittsburgh, PA, 1995.
(93) Frisch, M. J.; Trucks, G. W.; Schlegel, H. B.; Scuseria, G. E.; Robb, M. A.; Cheeseman, J. R.; Zakrzewski, V. G.; Montgomery, J. A.; Stratmann, R. E.; Burant, J. C.; Dapprich, S.; Millam, J. M.; Daniels, A. D.; Kudin, K. N.; Strain, M. C.; Farkas, O.; Tomasi, J.; Barone, V.; Cossi, M.; Cammi, R.; Mennucci, B.; Pomelli, C.; Adamo, C.; Clifford, S.; Ochterski, J.; Petersson, G. A.; Ayala, P. Y.; Cui, Q.; Morokuma, K.; Malick, D. K.; Rabuck, A. D.; Raghavachari, K.; Foresman, J. B.; Cioslowski, J.; Ortiz, J. V.; Stefanov, B. B.; Liu, G.; Liashenko, A.; Piskorz, P.; Komaromi, I.; Gomperts, R.; Martin, R. L.; Fox, D. J.; Keith, T.; Al-Laham, M. A.; Peng, C. Y.; Nanayakkara, A.; Gonzalez, C.; Challacombe, M.; Gill, P. M. W.; Johnson, B. G.; Chen, W.; Wong, M. W.; Andres, J. L.; Head-Gordon, M.; Replogle, E. S.; Pople, J. A. *Gaussian 98*, Revision A.1; Gaussian Inc.: Pittsburgh, PA, 1998.
(94) Hariharan, P. C.; Pople, J. A. *Theor. Chim. Acta* **1973**, *28*, 213−222.
(95) Becke, A. D. *J. Chem. Phys.* **1993**, *98*, 5648−5652.
(96) Møller, C.; Plesset, M. A. *Phys. Rev.* **1934**, *46*, 618−622.
(97) Johnson, B. G.; Gill, P. M. W.; Pople, J. A. *J. Chem. Phys.* **1993**, *98*, 5612−5626.
(98) Pople, J. A.; Headgordon, M.; Raghavachari, K. *J. Chem. Phys.* **1987**, *87*, 5968−5975.
(99) Reed, A. E.; Curtiss, L. A.; Weinhold, F. *Chem. Rev.* **1988**, *88*, 899−926.
(100) Reed, A. E.; Weinstock, R. B.; Weinhold, F. *J. Chem. Phys.* **1985**, *83*, 735−746.
(101) Glendening, E. D.; Reed, A. E.; Carpenter, J. E.; Weinhold, F. *NBO* Version 3.1.
(102) Erlebacher, J.; Carrell, H. L. ICRVIEW—Graphics program for use on Silicon Graphics computers from The Institute for Cancer Research, Fox Chase Cancer Center, Philadelphia, PA, 1992.
(103) Carrell, H. L. BANG—Molecular geometry program. The Institute for Cancer Research, Fox Chase Cancer Center, Philadelphia, PA 1976.
(104) Pople, J. A.; Headgordon, M.; Fox, D. J.; Raghavachari, K.; Curtiss, L. A. *J. Chem. Phys.* **1989**, *90*, 5622−5629.
(105) Curtiss, L. A.; Jones, C.; Trucks, G. W.; Raghavachari, K.; Pople, J. A. *J. Chem. Phys.* **1990**, *93*, 2537−2545.
(106) Vosko, S. H.; Wilk, L.; Nusair, M. *Can. J. Phys.* **1980**, *58*, 1200−1211.
(107) Perdew, J. P.; Zunger, A. *Phys. Rev. B* **1981**, *23*, 5048−5079.
(108) Burke, K.; Perdew, J. P.; Wang, Y. In *Electronic Density Functional Theory*; Dobson, J. B., Vignale, G., Das, M. P., Eds.; Plenum Press: 1998.
(109) Pederson, M. R.; Jackson, K. A. *Phys. Rev. B* **1990**, *41*, 7453−7461.
(110) Jackson, K.; Pederson, M. R. *Phys. Rev. B* **1990**, *42*, 3276−3281.
(111) Pederson, M. R.; Jackson, K. A. *Phys. Rev. B* **1991**, *43*, 7312−7315.
(112) Quong, A. A.; Pederson, M. R.; Feldman, J. L. *Solid State Commun.* **1993**, *87*, 535−539.
(113) Porezag, D.; Pederson, M. R. *Phys. Rev. B* **1996**, *54*, 7830−7836.
(114) Briley, A.; Pederson, M. R.; Jackson, K. A.; Patton, D. C.; Porezag, D. V. *Phys. Rev. B* **1998**, *58*, 1786−1793.
(115) Lee, C. T.; Yang, W. T.; Parr, R. G. *Phys. Rev. B* **1988**, *37*, 785−789.
(116) Miehlich, B.; Savin, A.; Stoll, H.; Preuss, H. *Chem. Phys. Lett.* **1989**, *157*, 200−206.

(117) Perdew, J. P.; Burke, K.; Ernzerhof, M. *Phys. Rev. Lett.* **1996**, *77*, 3865−3868.
(118) Perdew, J. P.; Burke, K.; Ernzerhof, M. *Phys. Rev. Lett.* **1997**, *78*, 1396.
(119) Del Bene, J. E.; Person, W. B.; Szczepaniak, K. *J. Phys. Chem.* **1995**, *99*, 10705−10707.
(120) Tsai, C. J.; Jordan, K. D. *J. Chem. Phys.* **1991**, *95*, 3850−3853.
(121) Tsai, C. J.; Jordan, K. D. *J. Phys. Chem.* **1993**, *97*, 5208−5210.
(122) Tsai, C. J.; Jordan, K. D. *Chem. Phys. Lett.* **1993**, *213*, 181−188.
(123) Kim, K.; Jordan, K. D.; Zwier, T. S. *J. Am. Chem. Soc.* **1994**, *116*, 11568−11569.
(124) Xantheas, S. S.; Dunning, T. H. *J. Chem. Phys.* **1993**, *98*, 8037−8040.
(125) Xantheas, S. S.; Dunning, T. H. *J. Chem. Phys.* **1993**, *99*, 8774−8792.
(126) Estrin, D. A.; Paglieri, L.; Corongiu, G.; Clementi, E. *J. Phys. Chem.* **1996**, *100*, 8701−8711.
(127) Sim, F.; Stamant, A.; Papai, I.; Salahub, D. R. *J. Am. Chem. Soc.* **1992**, *114*, 4391−4400.
(128) Laasonen, K.; Csajka, F.; Parrinello, M. *Chem. Phys. Lett.* **1992**, *194*, 172−174.
(129) Merrill, G. N.; Gordon, M. S. *J. Phys. Chem. A* **1998**, *102*, 2650−2657.
(130) Viant, M. R.; Brown, M. G.; Cruzan, J. D.; Saykally, R. J.; Geleijns, M.; van der Avoird, A. *J. Chem. Phys.* **1999**, *110*, 4369−4381.
(131) Saebo, S.; Tong, W.; Pulay, P. *J. Chem. Phys.* **1993**, *98*, 2170−2175.
(132) Reimers, J.; Watts, R.; Klein, M. *J. Chem. Phys.* **1982**, *64*, 95−114.
(133) Feyereisen, M. W.; Feller, D.; Dixon, D. A. *J. Phys. Chem.* **1996**, *100*, 2993−2997.
(134) Schutz, M.; Brdarski, S.; Widmark, P. O.; Lindh, R.; Karlstrom, G. *J. Chem. Phys.* **1997**, *107*, 4597−4605.
(135) Dyke, T. R.; Mack, K. M.; Muenter, J. S. *J. Chem. Phys.* **1977**, *66*, 498−510.
(136) Curtiss, L. A.; Frurip, D. J.; Blander, M. *J. Chem. Phys.* **1979**, *71*, 2703−2711.
(137) Simon, S.; Duran, M.; Dannenberg, J. J. *J. Phys. Chem. A* **1999**, *103*, 1640−1643.
(138) Wales, D. J. *J. Am. Chem. Soc.* **1993**, *115*, 11180−11190.
(139) Walsh, T. R.; Wales, D. J. *J. Chem. Soc., Faraday Trans.* **1996**, *92*, 2505−2517.
(140) Rodriguez-Cruz, S. E.; Jockusch, R. A.; Williams, E. R. *J. Am. Chem. Soc.* **1999**, *121*, 8898−8906.
(141) Bol, W.; Gerrits, G. J. A.; Panthaleon, v.; van Eck, C. L. *J. Appl. Crystallogr.* **1970**, *3*, 486-492.
(142) Caminiti, R.; Licheri, G.; Piccaluga, G.; Pinna, G. *Chem. Phys. Lett.* **1977**, *47*, 275−278.
(143) Waizumi, K.; Tamura, Y.; Masuda, H.; Ohtaki, H. *Z. Naturforsch.* **1991**, *A46*, 307−312.
(144) Caminiti, R.; Magini, M. *Chem. Phys. Lett.* **1979**, *61*, 40−44.
(145) Caminiti, R.; Marongiu, G.; Paschina, G. *Z. Naturforsch.* **1982**, *37*, 581−586.
(146) Cody, V.; Hazel, J. *Acta Crystallogr.* **1977**, *B33*, 3180−3184.
(147) Julian, M. O.; Day, V. W.; Hoard, J. L. *Inorg. Chem.* **1973**, *12*, 1754−1757.
(148) Dubler, E.; Jameson, G. B.; Kopajtic, Z. *J. Inorg. Biochem.* **1986**, *26*, 1−21.
(149) Cingi, M. B.; Lanfredi, A. M. M.; Tiripicchio, A.; Bandoli, G.; Clemente, D. A. *Inorg. Chim. Acta* **1981**, *52*, 237−243.
(150) Riley, P. E.; Pecoraro, V. L.; Carrano, C. J.; Raymond, K. N. *Inorg. Chem.* **1983**, *22*, 3096−3103.
(151) Gupta, M. P.; Van Alsenoy, C.; Lenstra, A. T. H. *Acta Crystallogr.* **1984**, *C40*, 1526−1529.
(152) Vanhouteghem, F.; Lenstra, A. T. H.; Schweiss, P. *Acta Crystallogr.* **1987**, *B43*, 523−528.
(153) Barnes, J. C.; Weakley, T. J. R. *J. Chem. Soc., Dalton Trans.* **1976**, 1786−1790.
(154) Harrowfield, J. M.; Sharma, R. P.; Skelton, B. W.; Venugopalam, P.; White, A. H. *Aust. J. Chem.* **1998**, *51*, 775−783.
(155) Muthuraman, M.; Bordet, P.; Le Fur, Y. *Z. Kristallogr.−New Cryst. Struct.* **1999**, *214*, 527−528.
(156) Haiwon, L.; Lynch, V. M.; Guang, C.; Mallouk, T. E. *Acta Crystallogr.* **1988**, *C44*, 365−367.
(157) Meyer, H.-J.; Pickardt, J. *Z. Anorg. Allg. Chem.* **1988**, *560*, 185−190.
(158) Castellari, C.; Comelli, F.; Ottani, S. *Acta Crystallogr.* **1999**, *C55*, 1054−1056.
(159) Arranz Mascaros, P.; Cobo Domingo, J.; Godino Salido, M.; Gutierrez Valero, M. D.; Lopez Garzon, R.; Low, J. N. *Acta Crystallogr.* **2000**, *C56*, e4.
(160) Graf, M.; Stoeckli-Evans, H.; Whitaker, C.; Marioni, P.-A.; Marty, W. *Chimia* **1993**, *47*, 202−205.
(161) Kariuki, B. M.; Valim, J. B.; Jones, W.; King, J. *Acta Crystallogr.* **1994**, *C50*, 1665−1667.
(162) Dahan, F. *Acta Crystallogr.* **1974**, *B30*, 22−27.
(163) Rychlewska, U.; Radanovic, D. D.; Jevtovic, V. S.; Radanovic, D. J. *Polyhedron* **2000**, *19*, 1−5.
(164) Schier, A.; Gamper, S.; Muller, G. *Inorg. Chim. Acta* **1990**, *177*, 179−183.
(165) Johnson, C. K. *Acta Crystallogr.* **1965**, *18*, 1004−1018.
(166) Passer, E.; White, J. G.; Cheng, K. L. *Inorg. Chim. Acta* **1977**, *24*, 13−23.
(167) Talberg, H. J. *Acta Chem. Scand.* **1977**, *A31*, 37−46.
(168) Marquis, D.; Greiving, H.; Desvergne, J.-P.; Lahrahar, N.; Marsau, P.; Hopf, H.; Bouas-Laurent, H. *Liebigs Ann. Chem.* **1997**, 97−106.
(169) Geday, M. A.; De Munno, G.; Medaglia, M.; Anastassopoulou, J.; Theophanides, T. *Angew. Chem., Int. Ed. Engl.* **1997**, *36*, 511−513.
(170) Bach, I.; Kumberger, O.; Schmidbaur, H. *Chem. Ber.* **1990**, *123*, 2267−2271.
(171) Turel, I.; Leban, I.; Zupancic, M.; Bukovec, P.; Gruber, K. *Acta Crystallogr.* **1996**, *C52*, 2443−2445.
(172) Blank, G.; Rodrigues, M.; Pletcher, J.; Sax, M. *Acta Crystallogr.* **1976**, *B32*, 2970−2975.
(173) Neuman, M. A.; Steiner, E. C.; van Remoortere, F. P.; Boer, F. P. *Inorg. Chem.* **1975**, *14*, 734−740.
(174) Shakeri, V.; Haussuhl, S. *Z. Kristallogr.* **1992**, *198*, 169−170.
(175) Shkol′nikova, L. M.; Polyanchuk, G. V.; Poznyak, A. L.; Yashunskii, V. G.; Ilyukhin, A. B. *Koord. Khim.* **1991**, *17*, 626−634.
(176) Ojala, W. H.; Lu, L. K.; Albers, K. E.; Gleason, W. B.; Richardson, T. I.; Lovrien, R. E.; Sudbeck, E. A. *Acta Crystallogr.* **1994**, *B50*, 684−694.
(177) Harrowfield, J. M.; Skelton, B. W.; White, A. H. *Aust. J. Chem.* **1995**, *48*, 1333−1348.
(178) Haas, A.; Klare, C.; Betz, P.; Bruckmann, J.; Kruger, C.; Tsay, Y.-H.; Aubke, F. *Inorg. Chem.* **1996**, *35*, 1918−1925.
(179) Kebarle, P. *J. Phys. Chem.* **1998**, *102*, 9978−9985.
(180) Caminiti, R.; Pashina, G. *Chem. Phys. Lett.* **1981**, *82*, 487−491.
(181) Kheawsrikul, S.; Hannongbua, S. V.; Rode, B. M. *Z. Naturforsch.* **1991**, *A46*, 111−116.
(182) Jaguar 4.1, Schrodinger Incorporated, Portland, OR 2000.
(183) Knochenmuss, R.; Leutwyler, S. *J. Chem. Phys.* **1992**, 5233−5244.
(184) Faraday, M. *Quant. J. Sci. Lett. Arts* **1823**, *15*, 71−74.
(185) Pauling, L.; Marsh, R. E. *Proc. Natl. Acad. Sci. U.S.A.* **1952**, *38*, 112−118.
(186) Jeffrey, G. A. *Acc. Chem. Res.* **1969**, *2*, 344−352.
(187) Tsoucaris, G. In *Organic Solid State Chemistry*; Desiraju, G. R., Ed.; Elsevier: Amsterdam, 1987; Chapter 7, pp 207−270.
(188) Perdew, J. P. In *Electronic Structure of Solids '91*; Ziesche, P., Eschrig, H., Eds.; Akademie Verlag: Berlin, 1991; p 11.
(189) Perdew, J. P.; Chevary, J. A.; Vosko, S. H.; Jackson, K. A.; Pederson, M. R.; Singh, D. J.; Fiolhais, C. *Phys. Rev. B* **1992**, *46*, 6671−6687.
(190) Perdew, J. P.; Chevary, J. A.; Vosko, S. H.; Jackson, K. A.; Pederson, M. R.; Singh, D. J.; Fiolhais, C. *Phys. Rev. B* **1993**, *48*, 4978.
(191) Perdew, J. P.; Burke, K.; Wang, Y. *Phys. Rev. B* **1996**, *54*, 16533−16539.
(192) Adamo, C.; Barone, V. *J. Comput. Chem.* **1998**, *19*, 418−429.
(193) Curtiss, L. A.; Raghavachari, K.; Pople, J. A. *J. Chem. Phys.* **1993**, *98*, 1293−1298.
(194) Nyden, M. R.; Petersson, G. A. *J. Chem. Phys.* **1981**, *75*, 1843−1862.